

**ANALYSIS AND DEVELOPMENT OF GRID CONNECTED FRONT-END
AC TO DC CONVERTER USING VOLTAGE ORIENTED CONTROL (VOC)**

VIVIEN BALAN



**A report submitted in partial fulfilment of the requirements for the degree of
Electrical Engineering (Power Electronic and Drives)**

UNIVERSITI TEKNIKAL MALAYSIA MELAKA

**Faculty of Electrical Engineering
UNIVERSITI TEKNIKAL MALAYSIA MELAKA**

2018

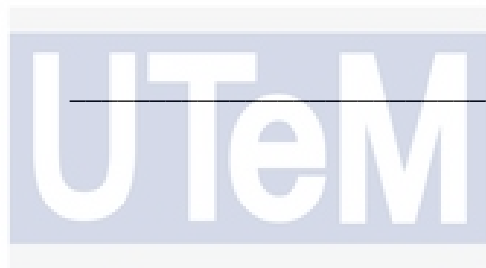
SUPERVISOR'S ENDORSEMENT

“I hereby declare that I have read through this report entitled “Analysis and development of Grid Connected Front-End AC to DC Converter Using Voltage Oriented Control (VOC)” and found that it complies the partial fulfilment for awarding the degree of Bachelor of Electrical Engineering”

Signature : _____

Supervisor's Name : DR. AZZIDDIN BIN MOHAMAD RAZALI

Date : _____



اونيورسيتي تيكنيكل مليسيا ملاك

UNIVERSITI TEKNIKAL MALAYSIA MELAKA

STUDENT DECLARATION

I declare that this report entitled “Analysis and Development of Grid Connected Front-End Ac to Dc Converter Using Voltage Oriented Control (VOC)” is the result of my own research except as cited in the references. The report has not been accepted for any degree and is not concurrently submitted in candidature of any other degree.

Signature : _____

Name : VIVIEN BALAN

Date : _____



DEDICATION

To my beloved mother and father
I will not complete without both of you



ACKNOWLEDGEMENT

In this moment, I would like to give big thanks and express my sincere appreciation to my supervisor, Dr. Azziddin bin Mohamad Razali, for his encouragement and guidance throughout this project. I was so grateful as he keeps on motivate and give advice that contribute to the completion of this report.

Besides, I would like to thank my beloved family as they support my project and until the end. Other than that, I am grateful to have my colleagues that help me with many ideas and tips on doing this project. Unfortunately, it is possible for me to list all of them in this limited space.

In a nutshell, I would like to thank both my panels, Dr. Zulhani Bin Rasin and En. Ahmad Aizan Bin Zulkefle, who gives great feedbacks and evaluation throughout my project. Through the both panels, I can improve my project in many aspects until I finish on doing my final year project.

ABSTRACT

This project is about the analysis and development of grid connected front end AC to DC converter using Voltage Oriented Control (VOC). Nowadays, the use of power electronic converters in industry are kept expanding. In industry, there is a problem in transmission and distribution lines as the harmonic and reactive currents are being injected into the system. Therefore, in electric power system, voltage control is important for proper operation for electrical power equipment. This is important to prevent any damage that might occur. Besides, the input current with non-sinusoidal shape drawn by conventional AC to DC converter generates significant harmonic components. The current harmonic components increase the current consumption and increase the power loss of utility equipment. As a result, overheating might happen in the generator and motor windings and the transmission line. One of the control methods for AC to DC converter is VOC. VOC controls the active and reactive power between grid and load by controlling approximately the three phase line currents and magnitude of the converter DC output voltage. Sinusoidal Pulse Width Modulation (SPWM) is used to determine the switching state of the converter. In addition, matrix transformations like Clarke Transformation, Park Transformation, Inverse Clarke Transformation and Inverse Park Transformation are used to simplify the development of the control method. The steady state performance and Total Harmonic Distortion (THD) of the line currents are analysed before and after the implementation of VOC method. The operation is kept at unity power factor with lower current THD. In a nutshell, by using VOC method, the three-phase input currents and voltages are almost in sinusoidal shape. Finally, a regulated DC power supply utilizing three-phase AC to DC converter can be constructed.

ABSTRAK

Projek ini adalah mengenai analisis dan perubahan terhadap grid yang bersambung dari hujung AC sampai ke hujung DC dengan menggunakan Kawalan Berorientasikan Voltan (VOC). Pada masa kini, penggunaan kuasa penukar eletronik dalam industri terus berkembang. Dalam industri ini, terdapat masalah dalam talian penghantaran dan pengedaran sebagai arus yang harmoni dan reaktif yang bersambung dalam sistem. Oleh itu, dalam sistem kuasa elektrik, kawalan voltan adalah penting untuk operasi yang betul untuk peralatan kuasa elektrik. Hal ini sangat penting bagi mengelakkan sebarang kerosakan yang mungkin berlaku. Selain itu, arus masuk dalam bentuk sinusoidal yang dibentuk oleh konvensional AC kepada penukar DC menghasilkan komponen harmoni yang ketara. Ini menyebabkan terdapat peningkatan terhadap voltan peralatan utiliti. Komponen harmoni semasa meningkatkan penggunaan semasa dan meningkatkan kehilangan kuasa peralatan utiliti. Akibatnya, pemanasan melampau mungkin berlaku di penjana dan litar motor dan talian penghantaran. Salah satu kaedah kawalan AC untuk penukar DC ialah VOC. VOC mengawal kuasa aktif dan reaktif antara grid dan beban dengan mengawal kira-kira arus tiga arus fasa dan magnitud voltan keluar penukar DC. Modulasi Lebar Pulse Sinusoidal (SPWM) digunakan dengan menggunakan fungsi MATLAB. Di samping itu, matrik transformasi seperti Transformasi Clarke, Transformasi Park, Transformasi Songsang Clarke dan Transformasi Songsang Park digunakan untuk mempermudah pembangunan kaedah kawalan. Kedudukan prestasi yang mantap dan Jumlah Masalah Harmoni (THD) arus elektrik dianalisis sebelum dan selepas pelaksanaan kaedah VOC. Operasi dikekalkan pada faktor kuasa satu dengan THD elektrik yang lebih rendah. Akhir sekali, dengan menggunakan kaedah VOC, arus dan tegangan masuk elektrik dan voltan tiga fasa hampir mencapai bentuk sinusoidal. Akhir sekali, bekalan kuasa DC yang dikawal menggunakan tiga fasa penukar AC ke DC boleh dibina.

TABLE OF CONTENT

	Page
ACKNOWLEDGEMENT	ii
ABSTRACT	iii
TABLE OF CONTENTS	v
LIST OF TABLES	viii
LIST OF FIGURES	ix
LIST OF SYMBOLS	xii
LIST OF APPENDICES	xiii
CHAPTER 1 INTRODUCTION	1
1.1 Project Background	1
1.2 Problem Statement	2
1.3 Objective	2
1.4 Scope of Research	3
1.5 Research Methodology	3
1.6 Report Outline	5
CHAPTER 2 LITERATURE REVIEW	6
2.1 Three Phase Bidirectional AC to DC Converter	6
2.2 Mathematical Model	8
2.3 Vector Transformation	9
2.3.1 Clarke Transformation	9
2.3.2 Park Transformation	10
2.3.3 Inverse Clarke Transformation	12
2.3.4 Inverse Park Transformation	12
2.4 Instantaneous Power	13

2.5	Control Strategies	14
2.5.1	Introduction	14
2.5.2	Voltage and Virtual Flux Oriented Control (VOC and VFOC)	15
2.5.3	Comparison and Discussion	16
2.6	Pulse Width Modulation (PWM)	18
2.6.1	Hysteresis Current Control PWM	19
2.6.2	Sinusoidal Pulse Width Modulation (SPWM)	20
2.6.3	Space Vector PWM	21
2.7	Phase Locked Loop	23
2.8	Development of current controller and voltage controller	25
2.8.1	Synchronous PI control	26
2.8.2	Development of current controller	26
2.8.3	Development of voltage controller	27
CHAPTER 3	ANALYSIS AND DEVELOPMENT OF VOLTAGE ORIENTED CONTROL (VOC)	28
3.1	Software Implementation	28
3.2	Block diagram	29
3.2.1	Development of Simulation Block Scheme	30
3.3	Subsystem Configuration	33
3.3.1	Clarke Transformation	33
3.3.2	Park Transformation	34
3.3.3	Phase Locked Loop (PLL)	35
3.3.4	MATLAB Function	37
3.3.5	Voltage Controller	38
3.3.6	Current Controller	39
3.3.7	Inverse Park Transformation	41
3.3.8	Inverse Clarke Transformation	42
3.3.9	Sinusoidal Pulse Width Modulation (SPWM)	43
CHAPTER 4	SIMULATION AND DISCUSSION OF RESULTS	44
4.1	Simulation of open loop rectifier	44

4.2	Simulation of three-phase AC to DC converter using VOC	51
4.3	Power Factor Operation Modes	55
4.4	Dynamic Performance	57
4.4.1	Load Variation	57
CHAPTER 5 CONCLUSION AND RECOMMENDATION		63
5.1	Conclusion	63
5.2	Recommendation on Future Work	64
REFERENCES		65
APPENDICES		63



LIST OF TABLES

Table	Title	Page
Table 2.1:	Comparison and Discussion of Control Strategies for Pulse Width Modulation (PWM) rectifier.	17
Table 2.2:	Commutation states of three-upper switch	22
Table 3.1:	Electrical Parameters for Simulation	33



LIST OF FIGURES

Figure	Title	Page
Figure 1.1:	Flowchart of Research Methodology	4
Figure 2.1:	Three-phase bidirectional AC-DC converter topology	7
Figure 2.2:	(a) Clarke Transformation from abc -coordinates to $\alpha\beta$ -coordinates for voltages	10
Figure 2.2:	(b) Clarke Transformation from abc -coordinates to $\alpha\beta$ -coordinates for currents	10
Figure 2.3:	Phasor Diagram of Park Transformation	11
Figure 2.4:	Phasor diagram of Inverse Clarke Transformation	12
Figure 2.5:	Phasor diagram of Inverse Park Transformation	13
Figure 2.6:	Control strategies	14
Figure 2.7:	(a) Block diagram of VOC	16
Figure 2.8:	Hysteresis current controller for phase “a”	19
Figure 2.9:	Hysteresis Band configuration	20
Figure 2.10:	diagram of SPWM	21
Figure 2.11:	SPWM basic waveforms	21
Figure 2.12:	Basic switching Voltage Vectors and Sector Division	22
Figure 2.13:	Switching for all vectors.	23
Figure 2.14:	Phase detector	24
Figure 2.15:	The PLL blocks	25
Figure 2.16:	Decoupled controller.	26
Figure 2.17:	Current control loop with PI controller.	27
Figure 2.18:	Voltage control loop with PI controller.	27
Figure 3.1	Block diagram for Voltage Oriented Control (VOC) [11].	29
Figure 3.2	Simulation Circuit Diagram of VOC.	31
Figure 3.3:	(a) Block diagram of Clark transformation for three-phase voltages. (b) Block diagram of Clarke transformation for three-phase currents.	34

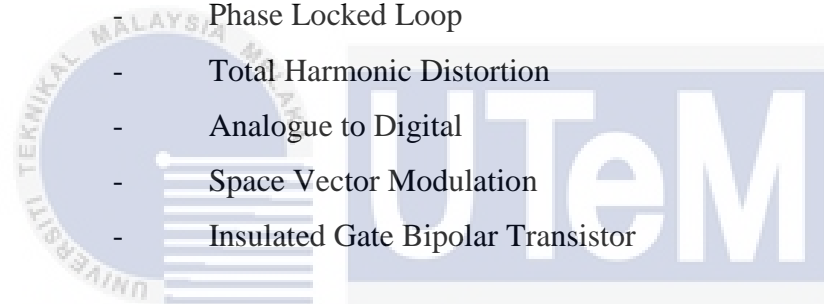
Figure 3.4: Block diagram of Park Transformation.	35
Figure 3.5: PLL Scheme.	36
Figure 3.6: Block diagram of PLL	36
Figure 3.7: PI controller with Voltage Control Loop.	38
Figure 3.8: Open loop voltage controller bode diagram.	39
Figure 3.9: PI controller with current control loop.	39
Figure 3.10: Open loop current controller bode diagram.	41
Figure 3.11: The block diagram of Inverse Park Transformation.	41
Figure 3.12: Block diagram of Inverse Clarke Transformation.	42
Figure 3.13: Simulink block of Sinusoidal Pulse Width Modulation.	43
Figure 4.1: Circuit of open loop rectifier.	44
Figure 4.2: Waveform of input voltages in abc -frame.	45
Figure 4.3: Waveform of input voltages in $\alpha\beta$ -frame.	45
Figure 4.4 Figure Waveform of input currents in abc -frame.	46
Figure 4.5 Waveform of input currents in $\alpha\beta$ -frame.	46
Figure 4.6: Voltage angle produced by $\text{atan}2$	47
Figure 4.7: Block diagram of PLL.	47
Figure 4.8: Voltage angle produced by $\text{atan}2$ and PLL.	47
Figure 4.9: Supply voltage in synchronously rotating dq reference frame.	48
Figure 4.10: Supply current in synchronously rotating dq reference frame.	48
Figure 4.11: frequency spectrum of grid current.	49
Figure 4.12: Waveform of Active power and Reactive power.	49
Figure 4.13: Generated dc-link output voltage.	50
Figure 4.14: Waveform of input voltages and generated dc-link output voltage.	50
Figure 4.15: Complete structure of VOC in MATLAB.	51
Figure 4.16: Three phase input current.	52
Figure 4.17: Phase a voltage and current at unity power factor.	52
Figure 4.18: Frequency spectrum of line current.	53
Figure 4.19: Supply current in synchronously rotating dq-reference frame.	53
Figure 4.20: Active and reactive powers of system.	54
Figure 4.21: DC-link output voltage with reference voltage.	54
Figure 4.22: Line current in dq-frame with $Q_{ref} = 100\text{Var}$	55
Figure 4.23: Phase a voltage and phase a current.	56

Figure 4.24: Line current in dq-frame with $Q_{ref} = -100\text{Var}$.	56
Figure 4.25: Phase a voltage with phase a current.	57
Figure 4.26: VOC with load variation	58
Figure 4.27: DC-link output voltage with $100\ \Omega$ of resistor in parallel.	59
Figure 4.28: Line current in rotating frame with $100\ \Omega$ in parallel.	59
Figure 4.29: Phase a current with $100\ \Omega$ in parallel.	60
Figure 4.30: Power flow of system with $100\ \Omega$ in parallel.	60
Figure 4.31: DC-link output voltage with $200\ \Omega$ of resistor in parallel.	61
Figure 4.32: Line current in rotating frame with $200\ \Omega$ in parallel.	61
Figure 4.33: Phase a current with $200\ \Omega$ in parallel.	62
Figure 4.34: Power flow of system with $200\ \Omega$ in parallel.	62



LIST OF SYMBOLS

VOC	-	Voltage Oriented Control
DPC	-	Direct Power Control
VFOC	-	Virtual Flux Oriented Control
VF-DPC	-	Virtual Flux Direct Power Control
PWM	-	Pulse Width Modulation
SPWM	-	Sinusoidal Pulse Width Modulation
PLL	-	Phase Locked Loop
THD	-	Total Harmonic Distortion
A/D	-	Analogue to Digital
SVM	-	Space Vector Modulation
IGBT	-	Insulated Gate Bipolar Transistor



اونيورسيتي تيكنيكل مليسيا ملاك
UNIVERSITI TEKNIKAL MALAYSIA MELAKA

LIST OF APPENDICES

APPENDIX	TITLE	PAGE
A	Gantt Chart	



CHAPTER 1

INTRODUCTION

1.1 Project Background

In industry, the harmonic pollution of power system is increased rapidly and reach a critical level that is beyond the tolerable limits. This pollution is mainly caused by nonlinear loads such as diode and thyristor rectifiers. There are several techniques can be used to reduce the harmonic pollution. There are from the application of active and passive filters and the use of Pulse Width Modulation (PWM) rectifiers. Throughout the studies, most of the researchers found out that PWM rectifiers have an additional advantage of the bi-directional power flow and hence PWM rectifiers becomes the best application amongst all.

Furthermore, the use of PWM rectifiers have presented four types of control techniques. Overall of control techniques can be distinguished as Voltage Oriented Control (VOC), Voltage-based Direct Power Control (V-DPC), Virtual-Flux Oriented Control (VFOC) and Virtual-Flux-based Direct Power Control (VF-DPC). For purpose of this study, a VOC is a method that been chosen for the analysis and development of grid connected front-end AC to DC converter.

Sinusoidal Pulse Width Modulation (SPWM) is used in VOC by properly control the pulses in the converter, thus assure the power flows are enough with stable frequency. The details of the process will be explained in this thesis. Other than that, VOC have no sensitive to line inductance variation with fixed switching frequency. Considering of all the advantages of VOC, VOC is one of the technique that can

overcome the rapid growth of ac adjustable speed drives (ASDs). Hence, VOC is the best method to convert from AC to DC.

1.2 Problem Statement

Power electronic systems are used wisely and very common usage in our daily life nowadays. Thus, same goes to AC to DC converter that are very common for most of us to hear about. However, there are problem that arise that might not be knowing by some of us when the converters are being connected in transmission and distribution lines. This problem is due to the harmonic and reactive currents that are injected into the system. The non-sinusoidal input currents that supply to the rectifier converter causes the significant harmonic components being generated. Finally, the volt-ampere rating of the utility equipment such as the transformers, generators and the transmission lines will then increase. A three-phase AC to DC converter can be controlled by a system known as the VOC scheme which produce a sinusoidal input current with a unity power factor.

1.3 Objective

The objectives are:

- i. To design a complete scheme of Voltage Oriented Control (VOC) using MATLAB Simulink.
- ii. To develop and test the control algorithm of the converter.
- iii. To analyse and study on the steady-state performance of three-phase diode rectifier

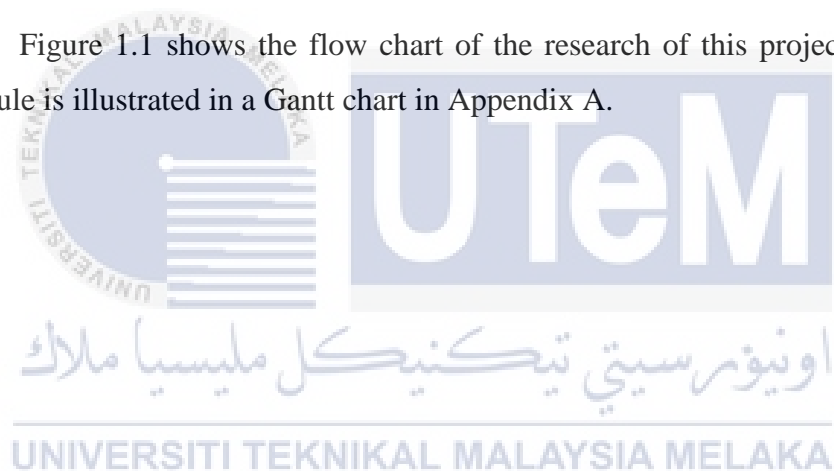
1.4 Scope of Research

The scopes of this project are:

- i. Design and simulate a complete VOC in MATLAB.
- ii. Obtain a lower Total Harmonic Distortion (THD) of grid current.
- iii. Able to obtain almost sinusoidal three-phase input current with almost unity power factor.
- iv. Achieving the DC output voltage that is close to the DC reference voltage.

1.5 Research Methodology

Figure 1.1 shows the flow chart of the research of this project. A complete schedule is illustrated in a Gantt chart in Appendix A.



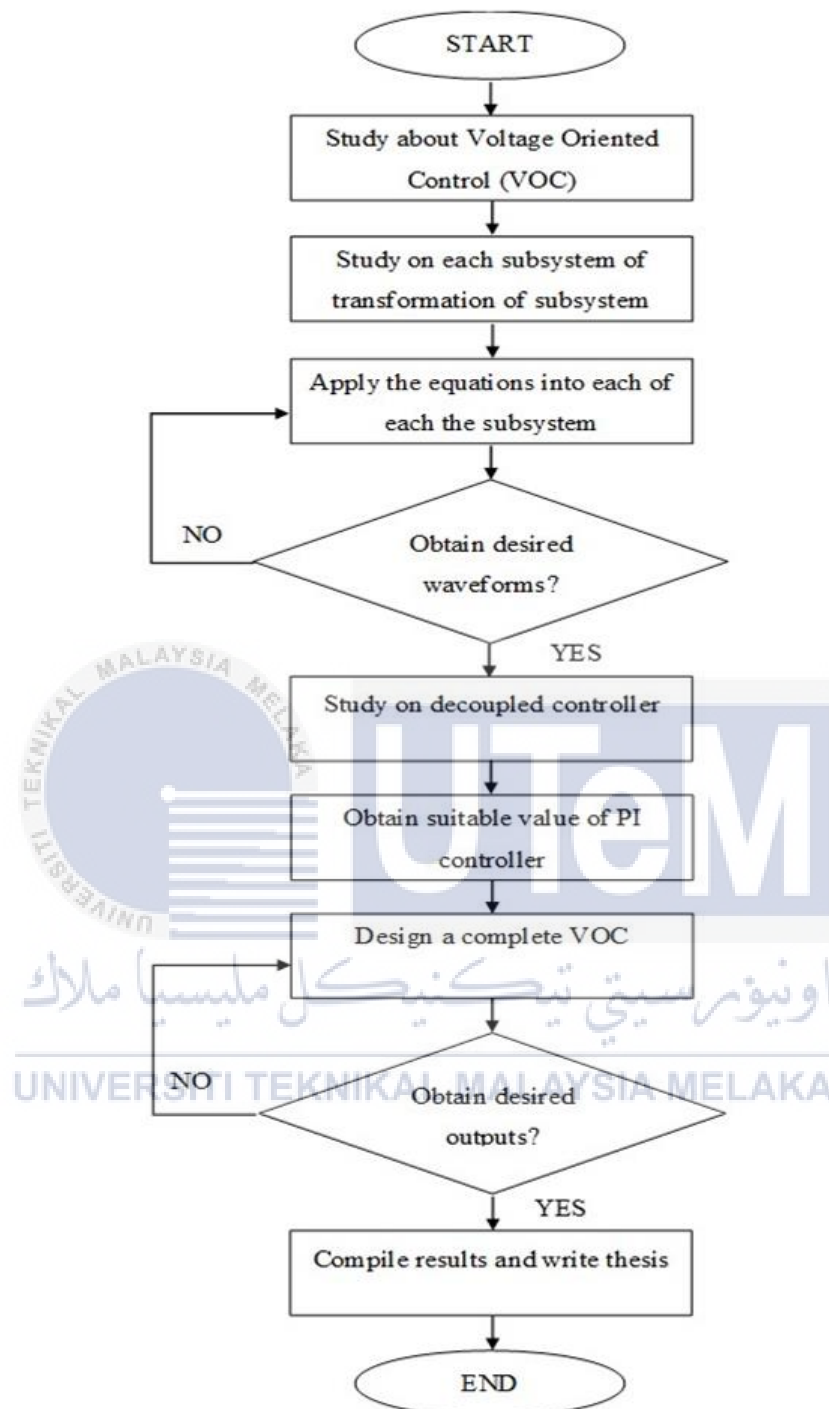


Figure 1.1: Flowchart of Research Methodology

1.6 Report Outline

In this report, there are six chapters as follows:

1. Chapter 1: Introduction
2. Chapter 2: Literature Review
3. Chapter 3: Analysis and Development of Voltage Oriented Control (VOC)
4. Chapter 4: Simulation Results and Discussions
5. Chapter 5: Conclusion and Recommendation.

In chapter 1, there are introduction that briefly describe about the design of the three-phase AC to DC converter. The objectives and the problem statements are described in this chapter. This will help to understand more and why is there needed to purpose and do this project. Besides, the flow of this project is shown as a guidance on doing and make the project more successful.

Chapter 2 is on the literature review that must be known and study before further on doing this project more deeply. Besides, through the fully understanding of the study, project becomes smoothly to work on. Other than that, the theory and calculations part are study to cover on the vector transformation, the control strategies and the mathematical modelling.

Chapter 3 covers the methodology being used to develop the regulated high voltage DC power supply utilizing the three-phase converter. All the models being use in order completing the design of VOC is shown this chapter. Thus, a complete simulation on VOC can be seen here.

All the simulation results of VOC are shown clearly in this chapter 4 with full explanations on each of the results which obtain from MATLAB Simulink. All the outputs and waveforms are organized to display the steady state and dynamic performance of the AC to DC converter either before nor after the introduction of VOC.

Lastly, this report is ended in chapter 5. In this chapter, it will summarise all the task been done in the project. Hence, there will be some recommendation in order having impressive performance of the project. Any future work for this project will be discuss in this chapter too.

CHAPTER 2

LITERATURE REVIEW

This chapter will review on research that been done by researches on Voltage Oriented Control (VOC). In the beginning, this thesis will start with an overview of three-phase controlled rectifiers. Next, will be move on to the mathematical modelling for each part of VOC, vector transformation, instantaneous power, control strategies and the Phase Locked Loop (PLL).

2.1 Three Phase Bidirectional AC to DC Converter

Higher harmonic content with lower of power factor effect the power distribution system. In order limiting the problems. Thus, there are new topologies that had been introduced for rectification applications. In this project, we will study on the most famous and universal topology, known as the universal bridge topology [1]. Through the analysis, three-phase voltage is connected to the two level of VSC. Basically, VSC consists of six insulated gates bipolar transistor (IGBT) with anti-parallel fast recovery diode.

Figure 2.1 shows the universal bridge topology which have the regulation of DC output voltage, low harmonic distortion of line current, near sinusoidal current waveforms, power factor correction, bidirectional power flow and unity power factor. The three-phase voltage is injected to each of the line inductors. A sinusoidal line currents and become the line filters by decrease the current ripples are the main function of the inductors.

The function of IGBTs is to boost the performance of the converter, where the IGBTs are suitable power switch as the gate driver can operates in high switching

frequency. The power switch can perform a continuous sinusoidal current from ac power supply with a lower Total Harmonic Distortion (THD) as mentioned before and minimum the grid needed for side power factor at unity in order obtaining the power transfer with a minimum current stress. In this project, the magnitude of V_{dc} need to be higher, where the minimum of DC link output voltage is required as of the equation (2.1).

$$V_{dc} > \sqrt{2} \times \sqrt{3} \times E_g, \text{ pahse, (rms)} = 2.45 \times E_g, \text{ pahse, (rms)} \quad (2.1)$$

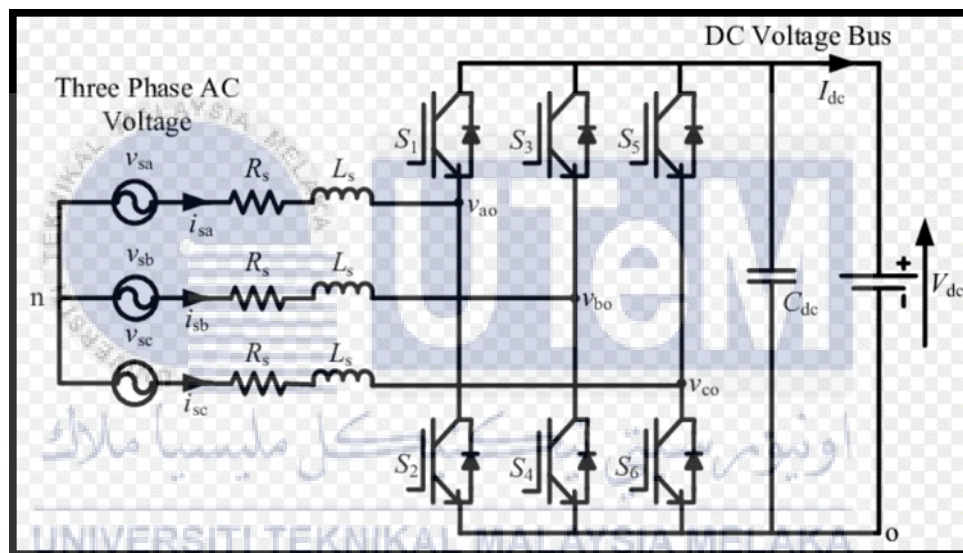


Figure 2.1: Three-phase bidirectional AC-DC converter topology

2.2 Mathematical Model

The three-phase line voltages and currents can be expressed in Equations (2.2) and (2.3) respectively as follow:

$$\begin{aligned} V_{sa} &= V_m \cos(\omega t) \\ V_{sb} &= V_m \cos\left(\omega t - \frac{2\pi}{3}\right) \\ V_{sc} &= V_m \cos\left(\omega t - \frac{4\pi}{3}\right) \end{aligned} \quad (2.2)$$

$$\begin{aligned} I_{sa} &= I_m \cos(\omega t + \varphi) \\ I_{sb} &= I_m \cos\left(\omega t + \varphi - \frac{2\pi}{3}\right) \\ I_{sc} &= I_m \cos\left(\omega t + \varphi - \frac{4\pi}{3}\right) \end{aligned} \quad (2.3)$$

With V_m as the input voltage and I_m as the input current. However, since that there is no neutral connection, the current can be obtained as Equation (2.4) below:

$$I_{m,sa} + I_{m,sb} + I_{m,sc} = 0 \quad (2.4)$$

Next, Equation (2.5) shows the voltages of each phase that can be determined and expressed as [2]

$$\begin{aligned} V_{\text{conv}, sa} &= (2S_a - S_b + S_c) \frac{V_{dc}}{3} \\ V_{\text{conv}, sb} &= (2S_b - S_a + S_c) \frac{V_{dc}}{3} \\ V_{\text{conv}, sc} &= (2S_c - S_a + S_b) \frac{V_{dc}}{3} \end{aligned} \quad (2.5)$$

The three-phase system are then described with only the two components which are α , the real part and β , the imaginary part.

2.3 Vector Transformation

2.3.1 Clarke Transformation

Clarke transformation is a transformation that can be expressed in the mathematical form. It is used to make the analysis less complex as the circuit for three-phase can be easily analysed for both voltage and current inputs. In this transformation, there are α and β as the components that represent and can be describe in the three-phase system the real and imaginary part respectively. The transformation of α and β are depending on Equations (2.6) and (2.7), where K is the constant [2]

$$V_s(t) = V_\alpha(t) + jV_\beta(t) \quad (2.6)$$

$$V_s(t) = V_\alpha(t) + jV_\beta(t) = \frac{2}{3} K (V_a(t) + V_b(t)e^{j\frac{2\pi}{3}} + V_c(t)e^{j\frac{4\pi}{3}}) \quad (2.7)$$

The equation can be transform in matrix form as in Equations (2.6) and (2.7) where the transformation is between the abc-reference frame to stationary $\alpha\beta$ -reference frame.

$$\begin{bmatrix} X_\alpha \\ X_\beta \end{bmatrix} = \begin{bmatrix} \sqrt{\frac{2}{3}} \\ \sqrt{\frac{2}{3}} \end{bmatrix} \begin{bmatrix} 1 & -\frac{1}{2} & -\frac{1}{2} \\ 0 & \frac{\sqrt{3}}{2} & -\frac{\sqrt{3}}{2} \end{bmatrix} \begin{bmatrix} X_a \\ X_b \\ X_c \end{bmatrix} \quad (2.8)$$

$$\begin{bmatrix} E_{g,\alpha} \\ E_{g,\beta} \end{bmatrix} = R \begin{bmatrix} I_{g,\alpha} \\ I_{g,\beta} \end{bmatrix} + L \frac{d}{dt} \begin{bmatrix} I_{g,\alpha} \\ I_{g,\beta} \end{bmatrix} + \begin{bmatrix} V_{conv,\alpha} \\ V_{conv,\beta} \end{bmatrix} \quad (2.9)$$

Where;

- $E_{g,\alpha\beta}$ – Stationary reference frame for three phase voltage supply
- $I_{g,\alpha\beta}$ – Supply current phase
- $V_{conv,\alpha\beta}$ – Converter pole voltage

The Clarke transformation of voltage and current are illustrated in Figures 2.2 (a) and (b).

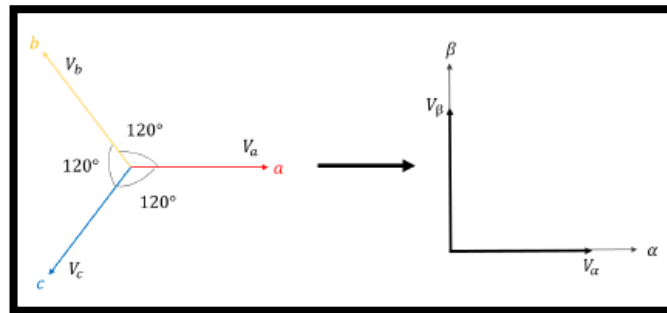


Figure 2.2(a) Clarke Transformation from abc -coordinates to $\alpha\beta$ -coordinates for voltages

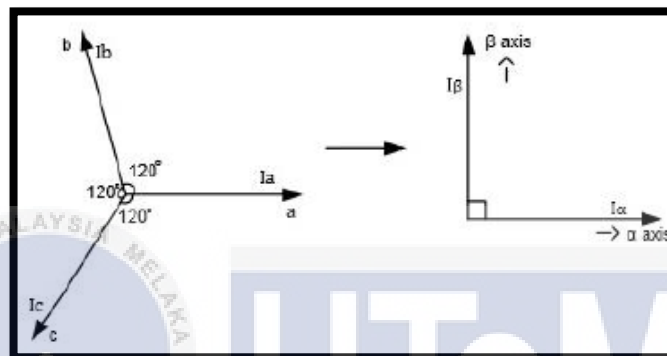


Figure 2.2 (b) Clarke Transformation from abc -coordinates to $\alpha\beta$ -coordinates for currents.

2.3.2 Park Transformation

Park transform or also known as dq transform is a space vector transformation. It transforms either voltage nor current of a stationary phase coordinate system into a rotating coordinate system of a three-phase time-domain signals. The dq-transformation can be shown in synchronous coordinates as in Equation (2.10). Figure 2.3 shows the transformation from $\alpha\beta$ -frame to dq-frame in form of phasor diagram.

$$V_{dq} = V_d + jV_q \quad (2.10)$$

2.3.3 Inverse Clarke Transformation

Inverse Clarke Transformation is a transformation from $\alpha\beta$ -coordinate to abc -coordinate. It is the transformation from two-phase voltages and currents into three-phase voltages and currents. The matrix shown in Equation (2.15) below shows the transformation being use. Figure 2.4 shows the phasor diagram of inverse Clarke transformation [3].

$$\begin{aligned} V_a &= V_\alpha \\ V_b &= \frac{-V_\alpha + \sqrt{3} + V_\beta}{2} \\ V_c &= \frac{-V_\alpha - \sqrt{3} + V_\beta}{2} \end{aligned} \quad (2.15)$$

Where,

V_a, V_b, V_c are three-phase quantities

V_α, V_β are stationary orthogonal reference frame quantities

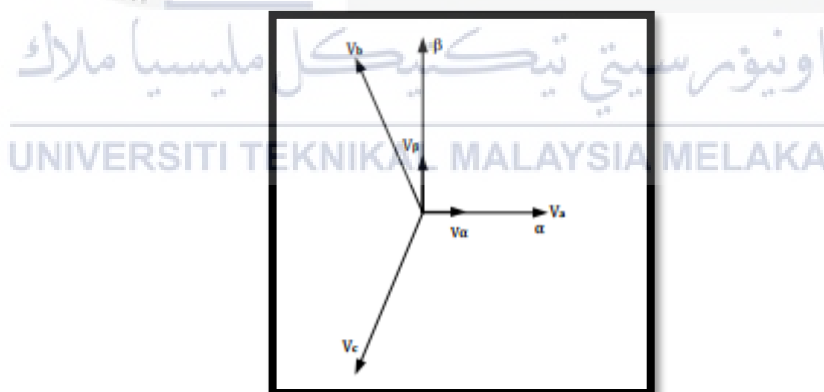


Figure 2.4: Phasor diagram of Inverse Clarke Transformation

2.3.4 Inverse Park Transformation

Inverse Park Transformation is the transformation from the rotating reference back to the stationary reference frame. Equation (2.16) and Figure 2.5 shows the transformation and the phasor diagram of inverse Park transformation respectively [3].

$$\begin{aligned}
 V_{\alpha} &= V_d * \cos (\theta) - V_q * \sin (\theta) \\
 V_{\beta} &= V_q * \cos (\theta) - V_d * \sin (\theta)
 \end{aligned}
 \tag{2.16}$$

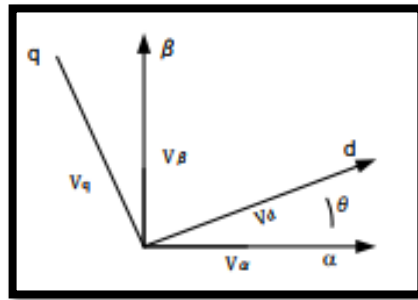


Figure 2.5: Phasor diagram of Inverse Park Transformation

2.4 Instantaneous Power

The Equation 2.17 is the common equation for power. In this project, after the vector transformation, the power exchange in dq reference is then given by Equation 2.18 together with the reactive power as in Equation 2.19. On the other hand, for the power exchange at DC side is equal to the power exchange at AC side as stated in Equation 2.20.

$$P = VI \tag{2.17}$$

$$\begin{aligned}
 P_{dq} &= \frac{3}{2} (V_d I_d + V_q I_q) \\
 &= \frac{3}{2} (V_{g,d} I_{g,d} + V_{g,q} I_{g,q})
 \end{aligned}
 \tag{2.18}$$

$$Q_{in} = \frac{3}{2} (V_{g,q} I_{g,d} - V_{g,d} I_{g,q}) \tag{2.19}$$

$$P_{dq} = P_{dc} = V_{dc} \times I_{dc} \tag{2.20}$$

Furthermore, the grid currents reference in dq, I_q , dq_{ref} when subtract to the grid currents, current error signals will be obtained. The Equations of (2.21) and (2.22) for reference current components which are $I_{g,d} \text{ ref}$ and $I_{g,q} \text{ ref}$ can be obtain from both the Equations (2.18) and (2.19).

$$I_{g,d \text{ ref}} = \frac{2}{3} \left[\frac{v_{g,d}}{v^2_{g,d} + v^2_{g,q}} \right] P_{\text{ref}} + \left[\frac{v_{g,d}}{v^2_{g,d} + v^2_{g,q}} \right] Q_{\text{ref}} \quad (2.21)$$

$$I_{g,q \text{ ref}} = \frac{2}{3} \left[\frac{v_{g,q}}{v^2_{g,d} + v^2_{g,q}} \right] P_{\text{ref}} - \left[\frac{v_{g,d}}{v^2_{g,d} + v^2_{g,q}} \right] Q_{\text{ref}} \quad (2.22)$$

2.5 Control Strategies

2.5.1 Introduction

The PWM rectifier are represented into two parts. There are the Voltage Based Control and the Virtual Flux Based Control. Figure 2.6 shows the sub-topic that can be discuss and compared. This is because of all the methods have almost similar outcomes or goals. The aim of those methods is having a unity power factor with waveform of the input currents are almost sinusoidal. Besides, there are also needing to have output voltage that is maintain at the required voltage [4].

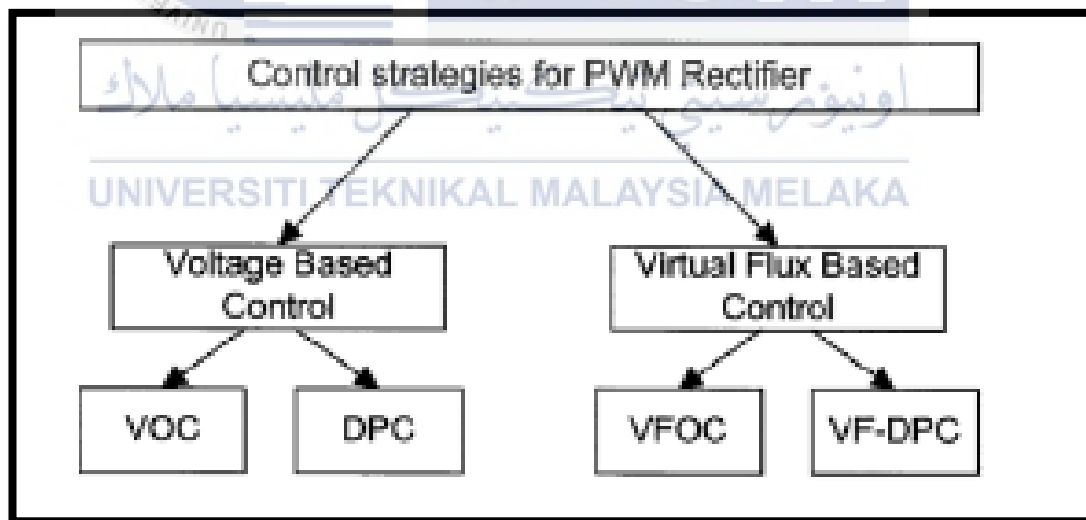


Figure 2.6: Control strategies

The four types of the technique can be distinguished:

- i. Voltage Oriented Control (VOC): Gives dynamic that is high enough with a static performance. This is obtained through the internal current control loop.
- ii. Direct Power Control (DPC): It is according to the instantaneous active power and the reactive power control loop. The switching state are determined with a switching table based on instantaneous errors between the commanded and estimated values of the active and reactive power.
- iii. Virtual Flux Based Control (VF-): It can be considered as a dual problem with vector control of an induction motor, IM. Other than that, it includes both the Virtual Flux Oriented Control (VFOC) and the Virtual Flux Direct Power Control (VF-DPC).

2.5.2 Voltage and Virtual Flux Oriented Control (VOC and VFOC)

VOC and VFOC are considered as the Field Oriented Control for induction motor. Basically, VOC and VFOC are about the transformation from the stationary coordinates $\alpha\beta$ to a synchronous rotating coordinates dq . By using these oriented control, there is an increase in rate of transient response and are directly improve the static performance through the internal current control loop.

A greater performance current control that are widely used is the dq synchronous controller. It is in DC quantities and are being able to eliminate the steady-state errors. In addition, VOC and VFOC are the best method such that the sampling frequency becomes lower and give a better performance as the A/D converters and the microcontroller are cheaper. Other than that, the switching frequency of VOC and VFOC are fixed and causes the input filter are easier to be design.

Under a non-ideal line voltage condition, VFOC can provide a changes and better performance for the rectifier control. However, for both VOC and VFOC, between the active and reactive components, there are coupling that occurs and some of the decoupling solution are needed. Finally, the coordinate transformation and PI controller are needed, which is also one of the disadvantages of using the VOC and VFOC. The details on VOC is shown in Figure 2.7 (a) and (b) [4].

Table 2.1: Comparison and Discussion of Control Strategies for Pulse Width Modulation (PWM) rectifier.

Control Strategies	Advantages	Disadvantages
VOC	<ul style="list-style-type: none"> • Switching frequency is fixed. • Can use advance PWM strategies • Cheap A/D converters. 	<ul style="list-style-type: none"> • Require coordinating transformation and decoupling between the active and reactive components. • Have a complicated process. • Have power factor lower than DPC.
DPC	<ul style="list-style-type: none"> • PWM block is not separated. • Does not need the coordinating transformation. • Have an uncomplicated process. • Better dynamics. • The power factor and efficiency are improved. 	<ul style="list-style-type: none"> • Sample frequency with high inductance is required. • The power and voltage should be prevented during the switching process. • Switching frequency is variable. • Require fast microprocessor and A/D converters.
VFOC	<ul style="list-style-type: none"> • Switching frequency is fixed. • Can use advance PWM strategies. • Cheaper A/D converters. • No sensitivity to line inductance variation. 	<ul style="list-style-type: none"> • Require coordinate transformation and decoupling between active and reactive components. • Complicated algorithm. • Less power factor compared to VF-DPC for the input power.

VF-DPC	<ul style="list-style-type: none"> • Sampling frequency is lower than V-DPC. • Have THD value for line currents that is lower. • Modulation block for the PWM voltage is combine. • Does not have the regulation loops for current and any coordinate transformation. • Dynamic performance is better. • Decoupled active and reactive power control. 	<ul style="list-style-type: none"> • Switching frequency is not fixed. • Require fast microprocessor and A/D converters.
--------	---	--

2.6 Pulse Width Modulation (PWM)

Pulse Width Modulation (PWM) is one of the way that can perform analogue results with digital means. In PWM, the square wave represents the digital control which represented in form of switch, either ON nor OFF. PWM can be apply in many electronic switching converters and inverters like the measurement and the communications for the control of power and the conversion.

PWM are important for controlling the DC motors. In any applications, PWM have its' own setting for the frequency where it is totally depending on how the powered system response. As a conclusion, PWM can reduces the switching losses and not difficult to implement and the computational time that needed is not too long. There are three techniques that are commonly used, which are hysteresis current control PWM, carrier based sinusoidal PWM and space vector PWM [6].

2.6.1 Hysteresis Current Control PWM

To develop the proposed switching control purpose, further understanding and study is made on the characteristic of the harmonic spectrum. There are more hysteresis band that have certain range with hysteresis switching mechanism that been arranged as it is important to achieve the desired switching frequency.

In this technique, the output current is pushing to follow the current phase reference signal. The command and the actual phase currents are compared, the current control is then performed the switching states for the converter to lower the errors that occur. Figure 2.8 shows the current error that occur for phase “a” which is limited by upper and lower band in hysteresis block [2].

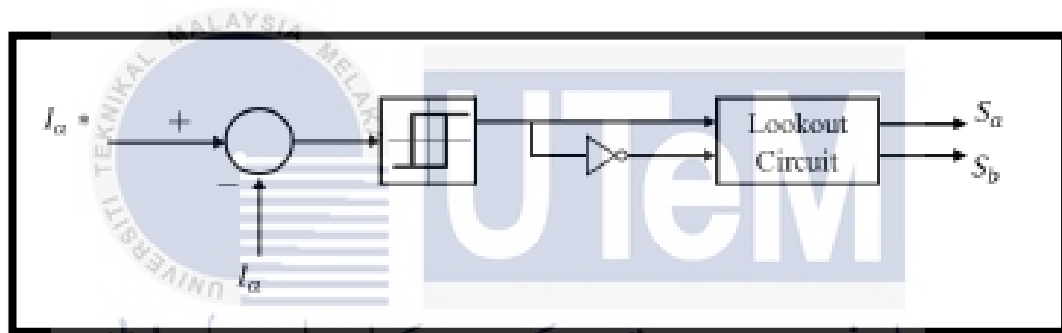


Figure 2.8: Hysteresis current controller for phase “a”

For further details, the increasing of current at upper band will cause the switch to be turning off to decrease the current until the lower limit that it can be reached. As the current is decrease, the switch is turning on again so that the current can be increasing to reach the upper limit. Hence, at same time, both the current control implements error and modulation. Figure 2.9 shows the results.

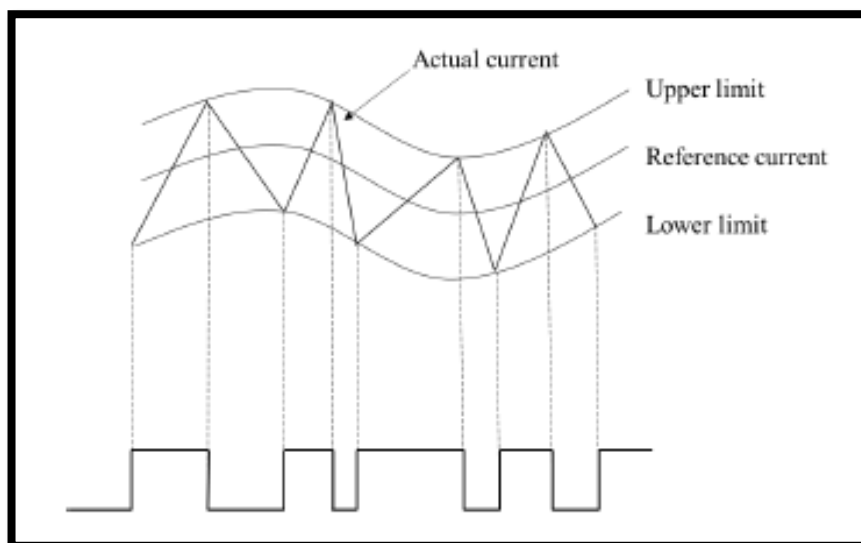


Figure 2.9: Hysteresis Band configuration

2.6.2 Sinusoidal Pulse Width Modulation (SPWM)

In Pulse Width Modulation (PWM), there are several techniques that can be implemented. The switching technique affects the total harmonic distortion and the switching losses. In this project, SPWM is used for which that it is not indirectly control for the DC output voltage and the three-phase input current. Figure 2.10 shows that there are three voltage inputs which represent the three sine waves that is compared with a high frequency triangular carrier wave. The sine waves which is also known as the reference signals have phase different of 120° between them. Frequency of 50Hz is chosen as the frequency of the reference signals, according to the grid voltage frequency, while the carrier signal frequency is set to 2050Hz. When a higher amplitude of sine wave compared to the triangular wave, it means that the comparator generates a high signal pulse. When the amplitude of the sine wave is lower than the triangular wave, then it is generating at a low signal pulse width. The gate pulses are used to trigger the IGBT switches ON and OFF. The basic waveform that should perform is shown in Figure 2.11.

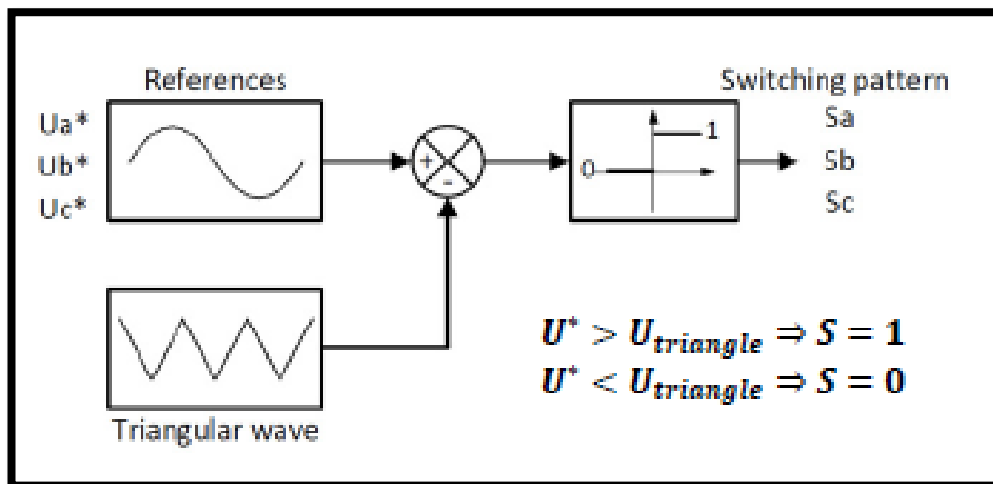


Figure 2.10: diagram of SPWM

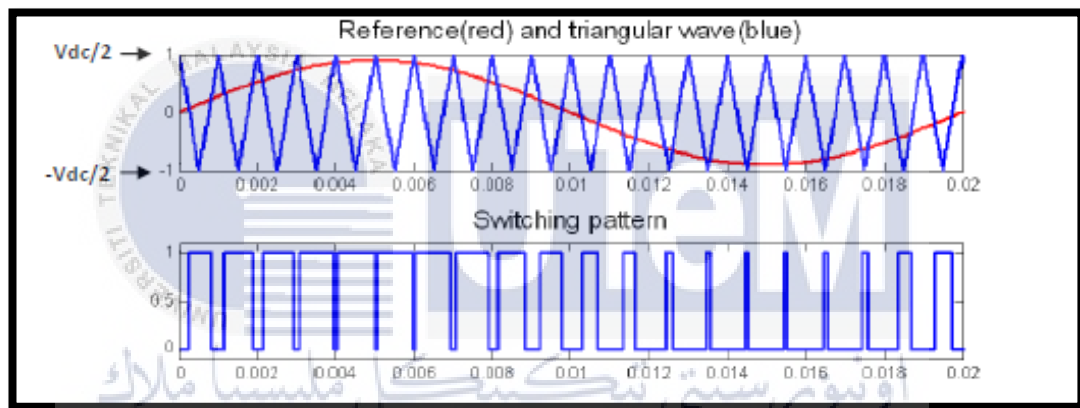


Figure 2.11: SPWM basic waveforms

2.6.3 Space Vector PWM

Space Vector PWM is one of the technique that is commonly used in industry. As compared to other methods, this space vector PWM is better where the computation-intensive is in elevated level of technology. In recent years, because of the superior performance characteristics of SVM, it has become the finding wide spread application. The switching state of the switches for each of the branch and leg are always opposite of each other and never be the same. Generally, the commutation states of the three-upper switches of rectifier are written as (S_a , S_b , S_c) of the commutation state vectors [8]. In SVM, vectors of six, which are the V_0 , V_1 , V_2 , V_3 , V_4 , V_5 , V_6 and the vector of two which are the V_0 and V_7 . Besides, in Table 2.2, it shows the eight possible converter configurations. Each of the vectors are illustrated in 60° and are represented in six sectors and was shown in Figure 2.12. The commutation

state of upper switches (S_a, S_b, S_c) for the eight vectors from V_0 to V_7 are shown in Figure 2.13.

Table 2.2: Commutation states of three-upper switch

Vector	Commutation state (S_a, S_b, S_c)
V_0	(000)
V_1	(100)
V_2	(110)
V_3	(010)
V_4	(011)
V_5	(001)
V_6	(101)
V_7	(111)

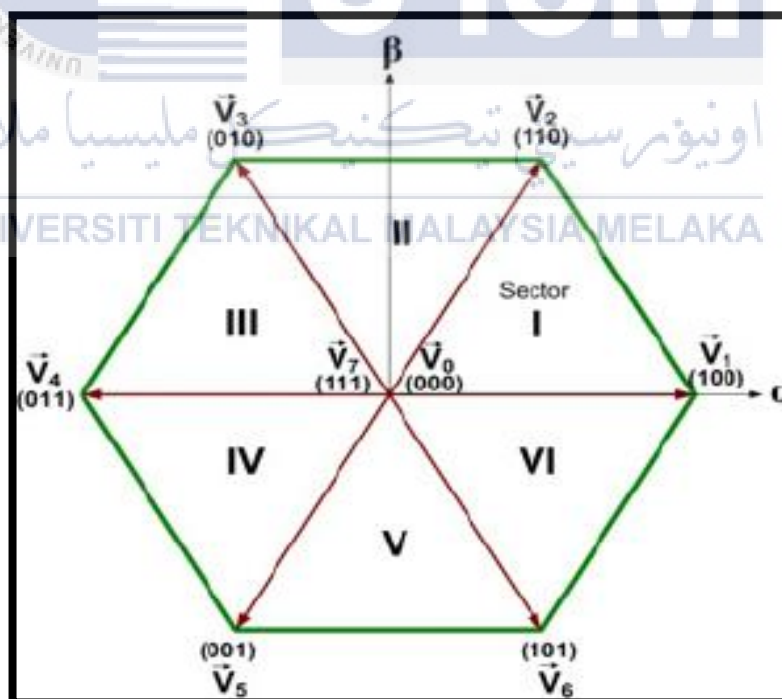


Figure 2.12: Basic switching Voltage Vectors and Sector Division

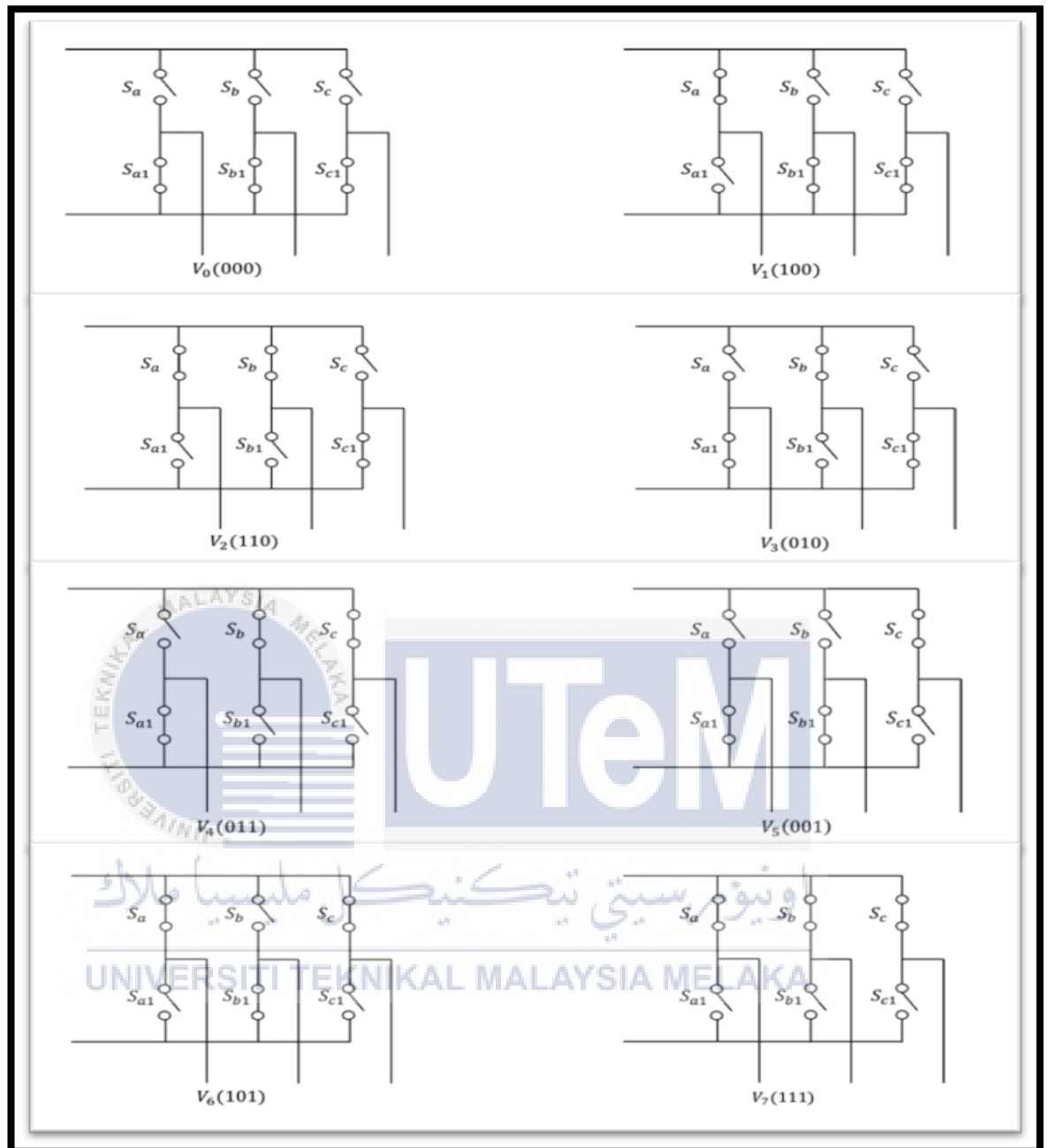


Figure 2.13: Switching for all vectors.

2.7 Phase Locked Loop

Phase Locked Loop (PLL), widely used in RF design, which considered as the master key for the designers to build the block. PLL are used in many ways for many things such as the FM demodulators, signal re-constitution, clock recovery and frequency synthesizers. PLL is based on the phase of signals and detects the phase difference between the signals. When the phase difference between the signals

changes, this means that they have difference in the frequencies. However, the frequencies are equal when the phase difference remains constant. This concept can be used in the PLL building blocks. In the loop, the main element will be the phase detector, PD, Voltage controlled oscillator, VCO and the loop filter.

The key element in the loop is the phase detector [9]. It takes two input signals, which are the reference signal and the signal from VCO to produce a signal that is the output voltage that is proportional to the phase difference. Figure 2.14 shows the flow on how the phase detector works. Besides, the next block is the VCO. Any number of oscillator circuits can be used to allow the Colpitts format. VCO is a simple oscillator that normally uses varactor diodes. It controls the terminal to which the control voltage is applied. Finally, there is the loop filter, which governs many of the loop characteristics. It is often a simple CR network that attenuates reference signal from the output. This shows the output shapes for the phase noise characteristic.

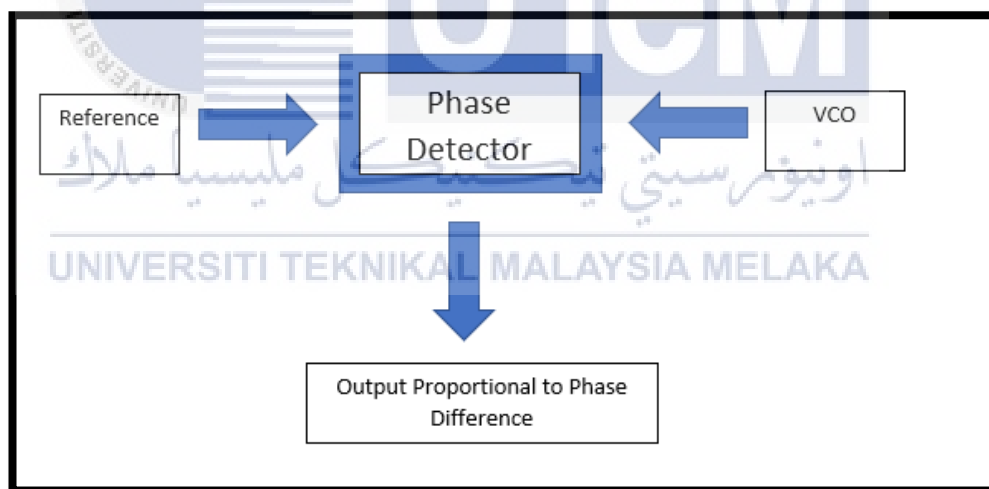


Figure 2.14: Phase detector

As a conclusion, these three main blocks are interconnected as shown in Figure 2.15. The input is taken from reference and VCO, which will give output that is directly proportional to the phase difference. Then, the different value for the voltage is then going through the loop filter. It is to need to decrease the frequency of the components. Next, the frequency is control by apply it on VCO. Any error for the voltage that occurs, which is found from phase detector will decrease the phase different of VCO

and the reference signals. It causes the frequency of VCO to be drawn onto the reference and having difference in steady state phase. The two signals that produced have the phase differenced that is constant. This shows that the VCO and the reference would have similar frequency and the loop is locked. It is important for VCO to have voltage that let it have the correct frequency, which means that there will always be a phase difference between the reference and the VCO.

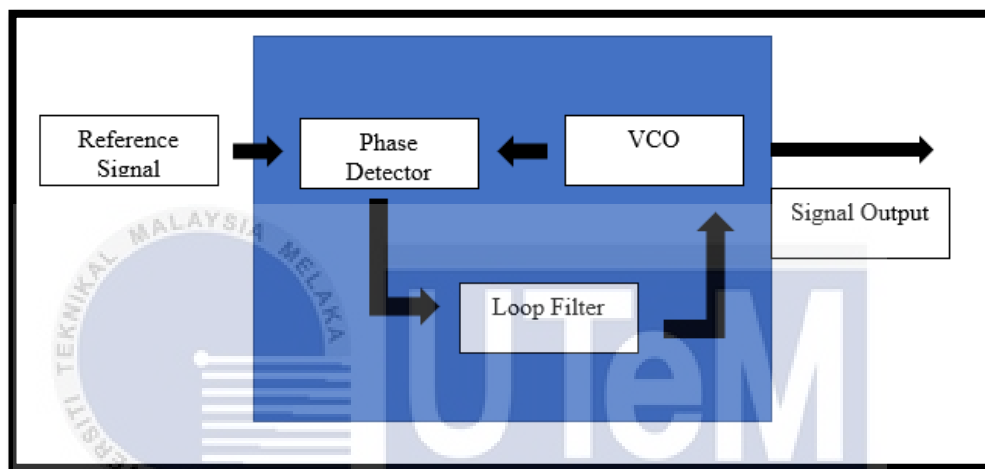


Figure 2.15: The PLL blocks

2.8 Development of current controller and voltage controller

The design of current controller is based on Internal Model Control (IMC). In this project, there will be decoupled control which with synchronous PI control. Figure 2.16 shows the diagram for a decouple controller. In addition, there will be one PI control act as voltage controller, while another two PI control will act as current controller.

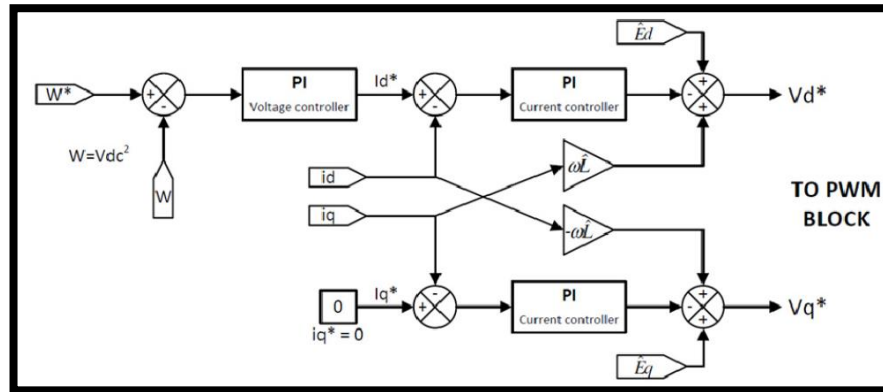


Figure 2.16: Decoupled controller.

2.8.1 Synchronous PI control

In order to prevent any steady state control error for the sinusoidal reference, PI control is used to overcome it. After the transformation, the dq measured current will be fed to PI current controller. As a result, there is an incredible dynamic response with better current tracking and the current controller shows less sensitivity to parameter variations [10]. Other than that, the output signal of the current controllers is shown in the Equations (2.23) and (2.24).

$$\Delta V_d = k_p (i_d^* - i_d) + k_i \int (i_d^* - i_d) dt \quad (2.23)$$

$$\Delta V_q = k_p (i_q^* - i_q) + k_i \int (i_q^* - i_q) dt \quad (2.24)$$

2.8.2 Development of current controller

As in Figure 2.17, it is the modified current control loop with PI controller. K_{RL} and T_{RL} are the line inductance and time constant respectively. The details of K_{RL} and T_{RL} are explained in Equation (2.25) and (2.26) below. In addition, K_{pc} and T_{IC} are based on Equation (2.27) and (2.28).

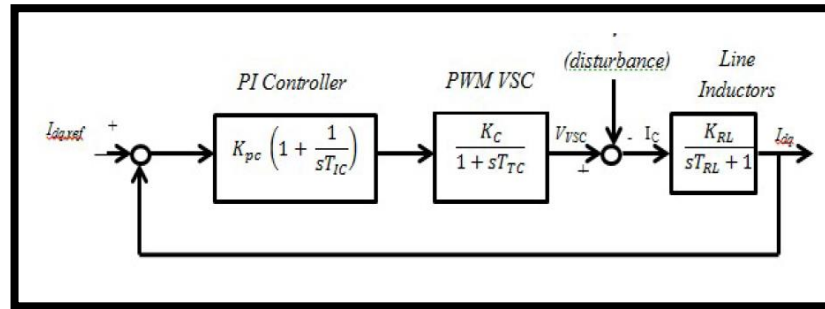


Figure 2.17: Current control loop with PI controller.

$$K_{RL} = \frac{1}{R} \quad (2.25)$$

$$T_{RL} = \frac{L}{R} \quad (2.26)$$

$$K_{RL} = \frac{T_{RL}}{2(T_s + T_{PWM} + T_d)} \quad (2.27)$$

$$T_{IC} = 4(T_s + T_{PWM} + T_d) \quad (2.28)$$

2.8.3 Development of voltage controller

Figure 2.18 shows the voltage control loop for PI controller. The power flow in the system becomes balance, while the DC output voltage of converter being regulated. Besides, Equations (2.29) and (2.30) are the equations being used for the development of voltage controller.

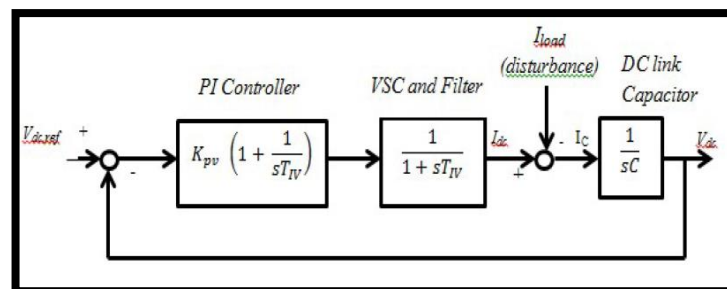


Figure 2.18: Voltage control loop with PI controller.

$$K_{PV} = \frac{C}{2T_{TV}} = \frac{C}{2(4T_{TC} + T_f)} \quad (2.29)$$

$$T_{TV} = 4T_{TV} = 4(4T_{TC} + T_f) \quad (2.30)$$

CHAPTER 3

ANALYSIS AND DEVELOPMENT OF VOLTAGE ORIENTED CONTROL (VOC)

In this chapter, it will focus more on the simulation part, where the subsystem for each block in VOC is design based on the equation that had been studied in chapter 2. Other than that, the project is then continue with the hardware implementation as the completion of simulation.

3.1 Software Implementation

MATLAB Simulink is being use in this project by starting with the construction of a three-phase full-bridge diode rectifier. Figure 3.1 shows the construction of the implemented of VOC, where the three-phase ac to dc converter utilizing IGBTs. The analysis for the dynamic and steady-state response of both the three-phase diode rectifier and converter is obtained.

3.2 Block diagram

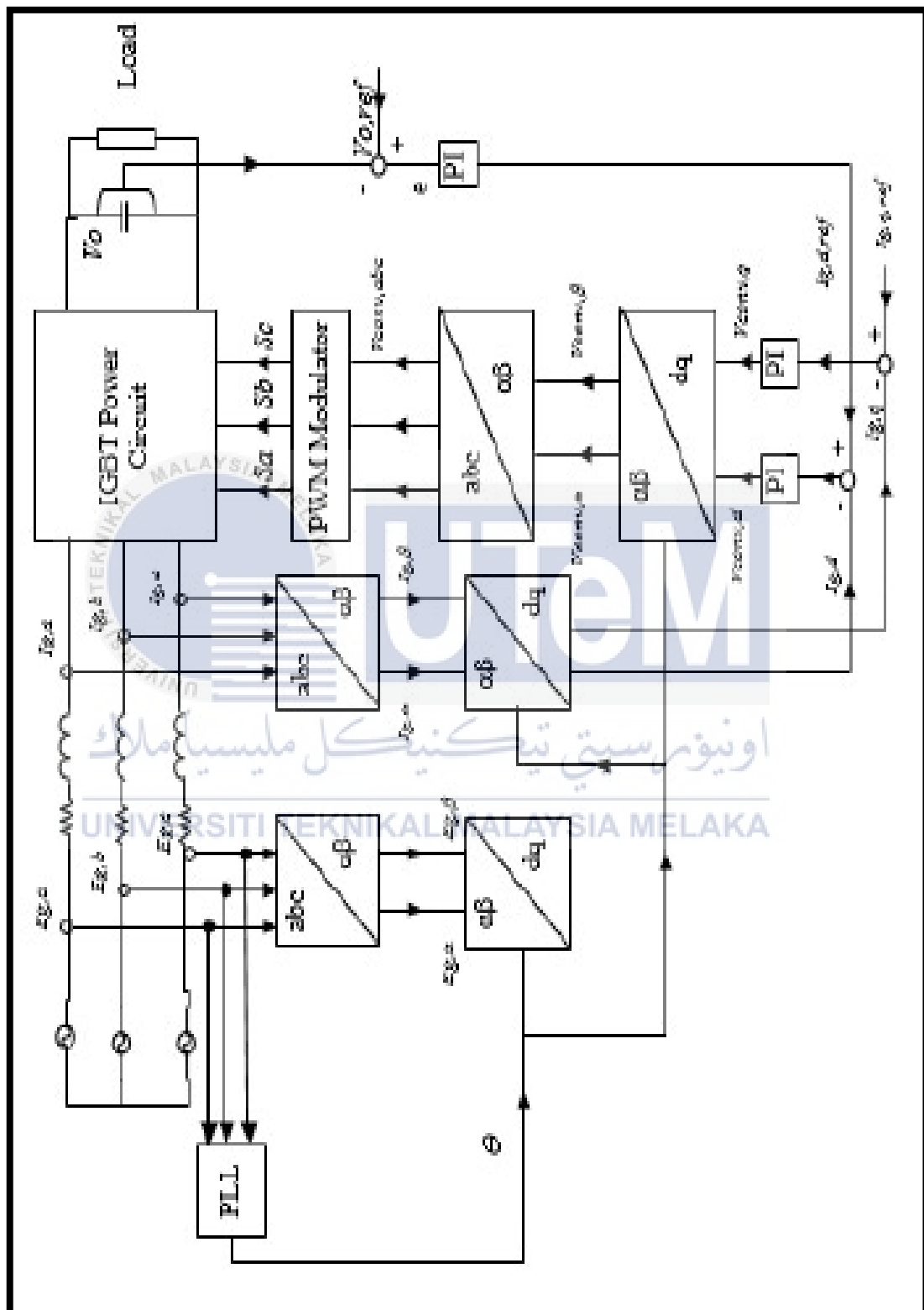


Figure 3.1 Block diagram for Voltage Oriented Control (VOC) [11].

Based on Figure 3.1, the diagram shows on how the three-phase AC to DC converter being used, where a pulse width modulation (PWM) AC-DC converter which is also known as the PWM rectifier, that is utilized to convert the AC voltage and current to DC voltage and current.

In the model for this project, there are four main parts, which are the Phase Locked Loop (PLL), a decoupled controller that composed by current and voltage controller, a PWM block and a rectifier model with the grid impedance R and L included. Besides, there are Voltage Oriented Control (VOC) in the dq-reference frame which to ensure that the system being able to produce excellent steady-state and dynamic performances.

There are internal current control loop and the outer voltage control loop which are the two control loops that contained by the VOC. As a basic principle, the VOC is a transformation between three-phase quantities to synchronous rotating coordinate, dq and stationary coordinate, $\alpha\beta$. The line voltages $E_{g,a}$, $E_{g,b}$ and $E_{g,c}$ are needed to feed the PLL and the voltage angle being calculated is used for the three-phase to dq-coordinate transformation of the line currents and voltages.

Furthermore, in a decoupled controller, there are also dq-coordinate values and the DC-link voltage value being used. Lastly, to create the switching patterns, all the reference voltages from the controller are sent to PWM block.

UNIVERSITI TEKNIKAL MALAYSIA MELAKA

3.2.1 Development of Simulation Block Scheme

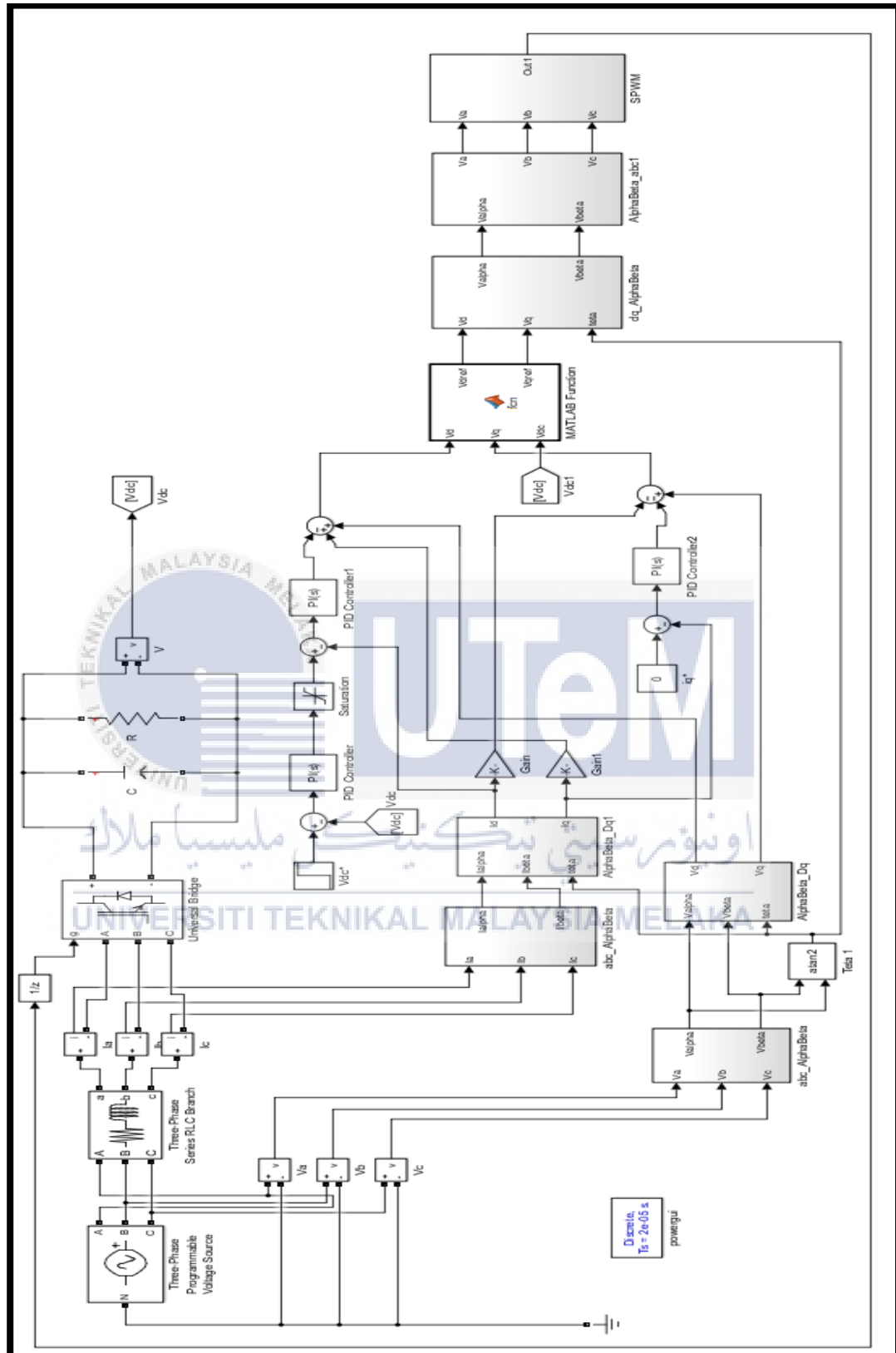


Figure 3.2 Simulation Circuit Diagram of VOC.

Figure 3.2 shows the complete structure of VOC in MATLAB. In the study, there are two types of converters, known as Voltage Source Converters (VSC) and Current Source Converters (CSC). Voltage fed converter is the VSC, while current fed converter is the CSC. VSC consists of Insulated Gate Bipolar Transistor (IGBT) that can be either turning on nor off in a controller manner [12]. The whole AC-DC converter system is constructed in discrete mode to study the performance in steady state and dynamic operation. The electrical parameters used in the simulation are shown in Table 3.1.



Table 3.1: Electrical Parameters for Simulation

Parameters	Values
Input phase voltage, E_g	70.71V
Source voltage frequency, f	50Hz
DC-Link voltage reference, $V_{dc}(\text{ref})$	150V
Resistance of reactance, R	0.2Ω
Inductance of reactance, L	15mH
DC-link capacitor, C	10.8mF
Load resistance, R_L	140Ω
Sampling time, f_s	20us

3.3 Subsystem Configuration

A process on constructing a full Simulink diagram of VOC that shown in Figure 3.2. There are a few subsystems block that need to be constructed. Through the simulation for each of the subsystem, there are a few important waveforms that need to be obtained. The waveforms are such as the three-phase inputs for current and voltage, the alpha-beta frame for current and voltage, the active and reactive powers and the DC output voltage. The x-axis and y-axis for the axes are adjusted to a suitable range with all the waveforms that captured using the time scope in MATLAB. The line graph of the waveform can be differentiated through colours by changing the “style” of the line.

3.3.1 Clarke Transformation

In the beginning, VOC is based on the transformation between stationary coordinates $\alpha\beta$ and synchronous rotating coordinates dq . This method causes the transient response to be faster with high static performance through internal current control loop. For the simulation, the abc -frame and $\alpha\beta$ -frame as the input voltage and current waveforms are obtained. Figure 3.3 (a) and (b) show the Clarke transformation, where the same subsystem was used for both the abc -frame of voltages and currents. The subsystem is build according to the Equations (3.1) and (3.2).

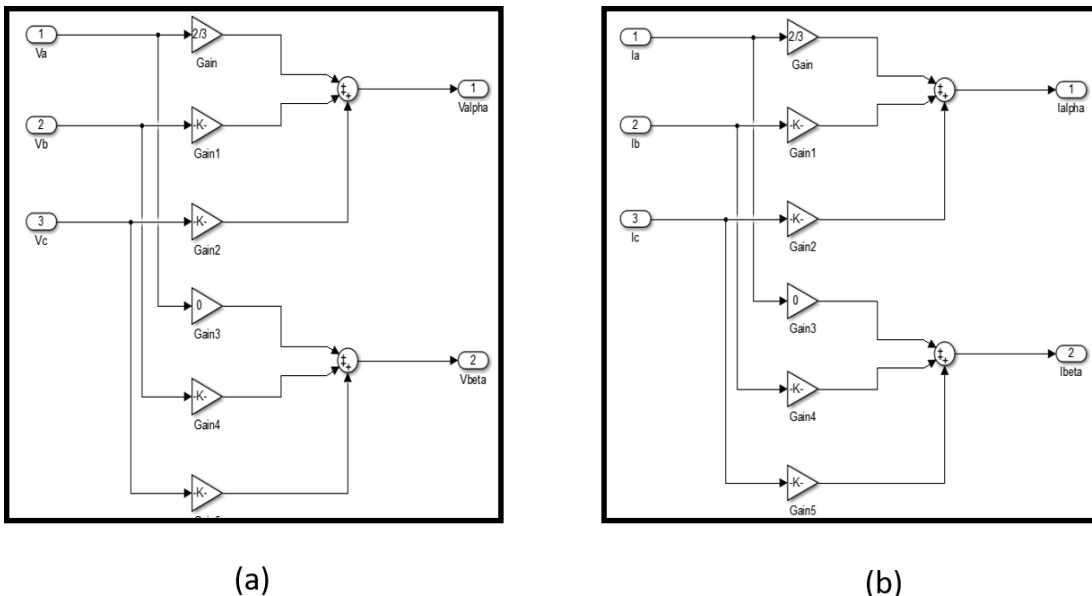
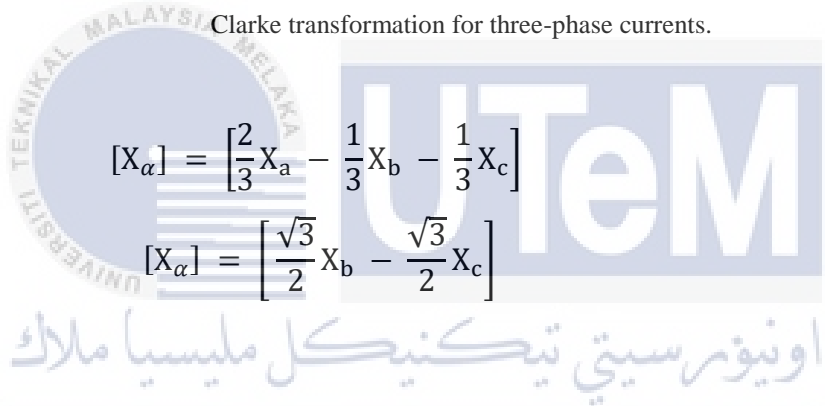


Figure 3.3: (a) Block diagram of Clark transformation for three-phase voltages. (b) Block diagram of Clarke transformation for three-phase currents.



$$[X_\alpha] = \left[\frac{2}{3} X_a - \frac{1}{3} X_b - \frac{1}{3} X_c \right] \tag{3.1}$$

$$[X_\alpha] = \left[\frac{\sqrt{3}}{2} X_b - \frac{\sqrt{3}}{2} X_c \right] \tag{3.2}$$

3.3.2 Park Transformation

Park Transformation is one of the subsystem that been used in Figure 3.2. Figure 3.4 shows the block diagram of Park Transformation. The transformation is depending on Equations (3.3) and (3.4) [3]. The transformation is the transformation from two phase voltages or currents into three phases.

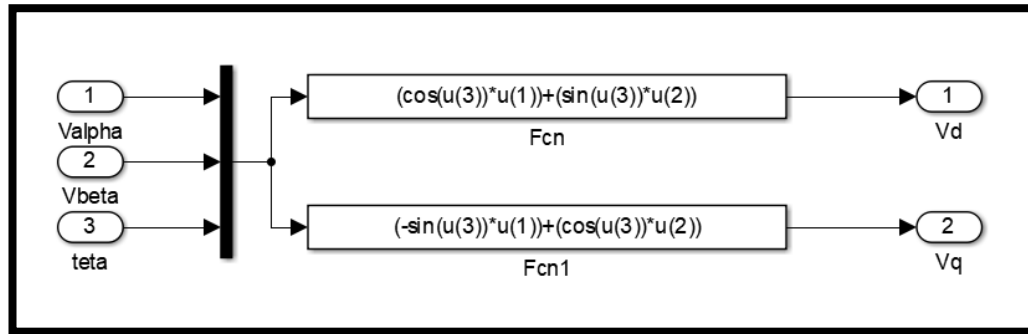


Figure 3.4: Block diagram of Park Transformation.

$$[X_d] = [\cos\theta + \sin\theta] [X_\alpha] \quad (3.3)$$

$$[X_q] = [-\sin\theta + \cos\theta] [X_\beta] \quad (3.4)$$

3.3.3 Phase Locked Loop (PLL)

Grid synchronization is an important feature of grid side converter control in order detecting the phase angle of grid voltage. Thus, the power been delivered will be synchronized too. PLL is used in order synchronizing the output current of the inverter with the grid voltage. Hence, we can now be obtaining unity power factor. The three-phase voltage measured, V_{sa} , V_{sb} and V_{sc} on the grid side, which act as the inputs of the PLL model, while the output of PLL model will be the tracked phase angle. Other than that, the tracked phase angle that obtained is then implemented in dq reference frame. Figure 3.5 and 3.6 shows the PLL scheme and block diagram of PLL respectively. In this project, the angle as the output of PLL that obtained are applied for both the voltage and current $\alpha\beta$ -frames. The subsystem of PLL was build based on Equation (3.5), where the Equation are then divide into Equations (3.6) and (3.7).

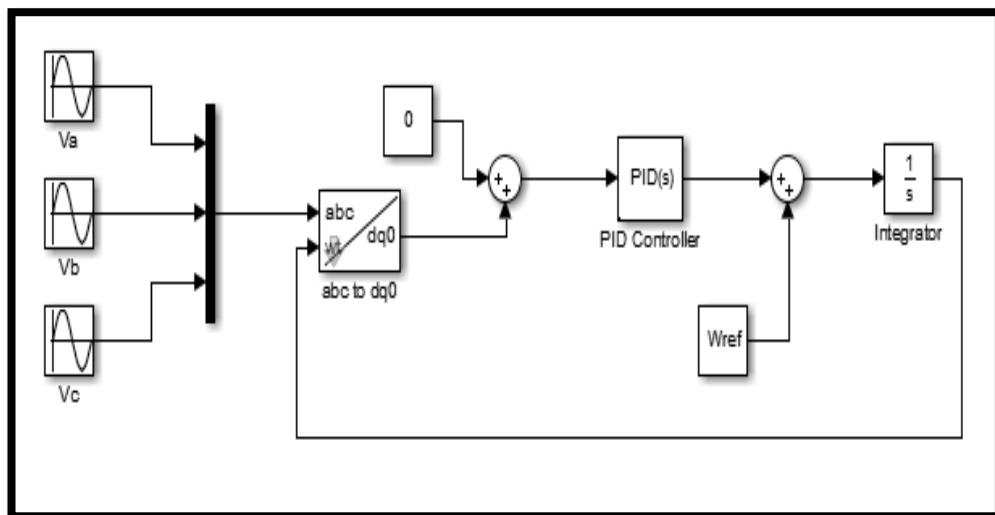


Figure 3.5: PLL Scheme.

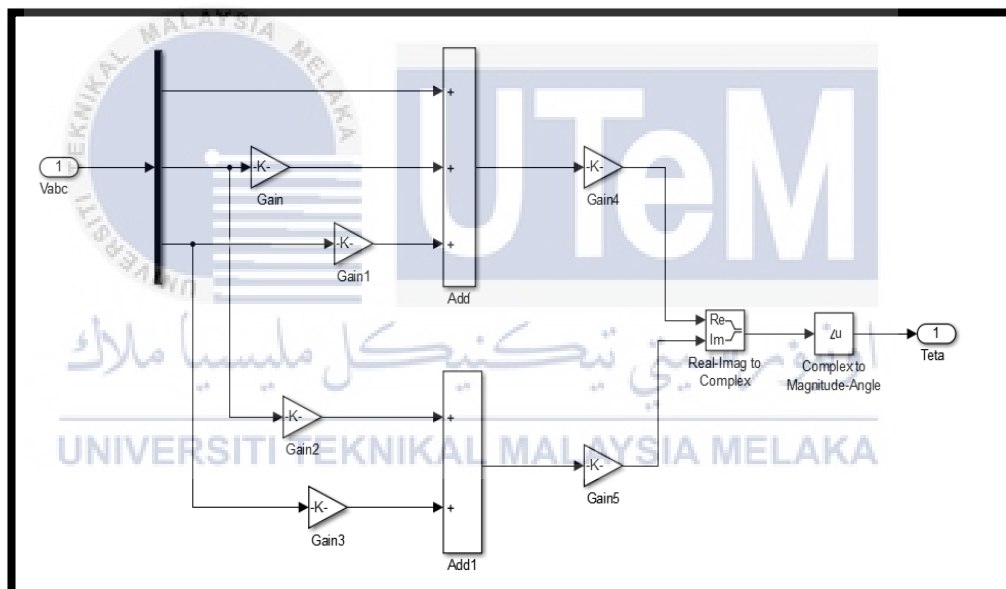


Figure 3.6: Block diagram of PLL

$$\begin{bmatrix} V_{\alpha} \\ V_{\beta} \end{bmatrix} = \begin{bmatrix} \sqrt{\frac{2}{3}} \\ 0 \end{bmatrix} \begin{bmatrix} 1 & -\frac{1}{2} & -\frac{1}{2} \\ 0 & \frac{\sqrt{3}}{2} & -\frac{\sqrt{3}}{2} \end{bmatrix} \begin{bmatrix} V_a \\ V_b \\ V_c \end{bmatrix} \quad (3.5)$$

$$V_{\alpha} = \theta_1 = \begin{bmatrix} \sqrt{\frac{2}{3}} \end{bmatrix} \left[V_a - \frac{1}{2} V_b - \frac{1}{2} V_c \right] \quad (3.6)$$

$$V_{\beta} = \theta_2 = \begin{bmatrix} \sqrt{\frac{2}{3}} \\ \frac{\sqrt{3}}{2} V_b - \frac{\sqrt{3}}{2} V_c \end{bmatrix} \quad (3.7)$$

3.3.4 MATLAB Function

Before obtaining the voltage converter of dq from the PI controller, the voltage converter need MATLAB function that limit or normalise the output voltage between +1V and -1V. The limitation can be done in the editor as shown below:

```
function [V_dref, V_qref] = fcn (V_d, V_q, V_dc)
%This block supports an embeddable subset of the MATLAB language.
%See the help menu for details.

V=(V_d*V_d+V_q*V_q) ^0.5;    %modulus voltage
% V_norm=V*(2/V_dc);        %normalized V (V/V_dcref/2))
V_norm=V*(1/V_dc);
V_n=V_norm;
Cos=V_d/V;
Sin=V_q/V;

%maxlimit=V_dc*0.5;
%minlimit=V_dc*0.5;

if (V_norm>=1)
    V_norm=1;
elseif (V_norm<=-1)
    V_norm=-1;
elseif ((V_norm<1) &&(V_norm>-1))
    V_norm=V_n;
end

V_dref=Cos*V_norm;

V_qref=Sin*V_norm;
```

As we can see, V_d , V_q and V_{dc} as the input for the MATLAB function. After the implementation, the output will be V_{dref} and V_{qref} . If the value of V_{norm} is greater or equal to 1V, then V_{norm} will equal to 1V. When V_{norm} less or equal to 1V, then $V_{norm} = -1$. Thus, if V_{norm} less or more than 1V, then V_{norm} will be equal to V_n .

3.3.5 Voltage Controller

Figure 3.7 shows the subsystem that been used in this project. The voltage controller is control by adjust or tune the value of K_{pv} and K_{iv} . This is very important as the system of PWM rectifier need to operate in a stable condition. Equations (3.8) to (3.13) shows the equation being used in order building the voltage control loop with PI controller.

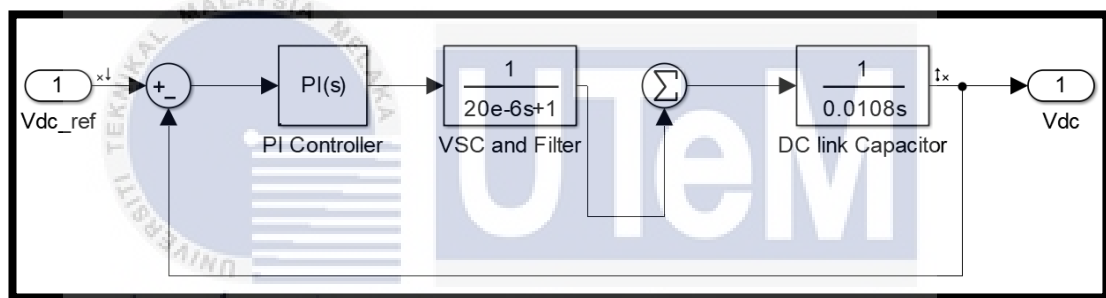


Figure 3.7: PI controller with Voltage Control Loop.

$$\text{PI Controller} = K_{PV} \left[1 + \frac{1}{sT_{IV}} \right] \quad (3.8)$$

$$\text{VSC and Filter} = \frac{1}{1 + sT_{IV}} \quad (3.9)$$

$$\text{DC link Capacitor} = \frac{1}{sC} \quad (3.10)$$

$$T_{TV} = 4T_{TC} + T_f \quad (3.11)$$

$$K_{PV} = \frac{C}{2T_{TV}} = \frac{C}{2(4T_{TC} + T_f)} \quad (3.12)$$

$$T_{IV} = 4T_{TV} = 4(4T_{TC} + T_f) \quad (3.13)$$

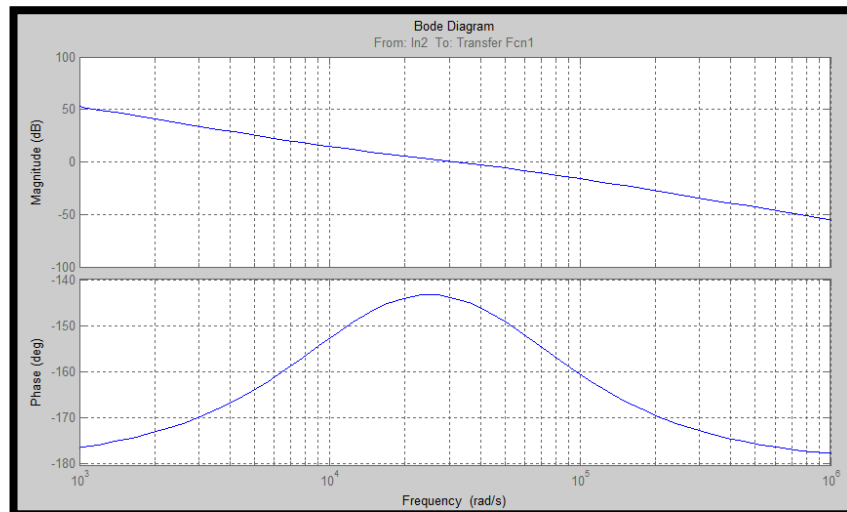


Figure 3.8: Open loop voltage controller bode diagram.

Figure 3.8 shows that the phase margin is 53.1° with 31600 rad per second or 187.87kHz. The bode diagram shows the negative infinity phase margin. Thus, the system is stable condition. Through the analysis, the open loop voltage controller has magnitude of -0.648dB, which is lower than the magnitude of open loop current controller with -0.701dB as shown in Figure. This is important to note that as it fulfil the criterion on having stable control system.

3.3.6 Current Controller

Figure 3.9 shows the transfer function of line inductor. This block diagram is analysed using parameters given in Table 3.1. The details equation on PI controller, PWM VSC and line inductors are explained in Equation (3.14) to (3.21).

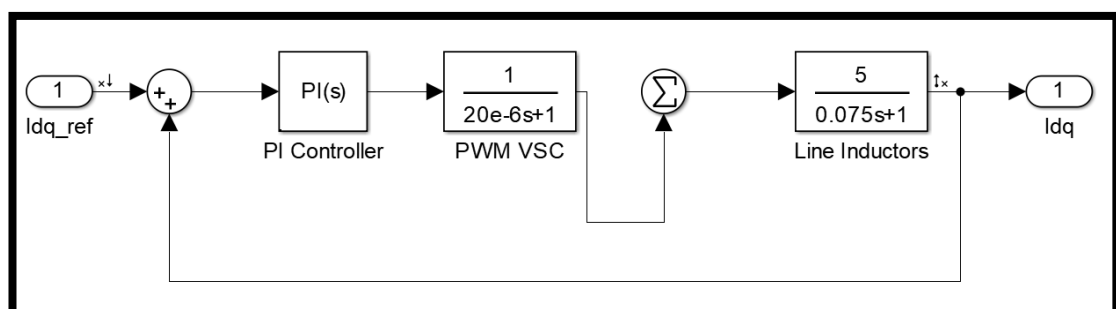


Figure 3.9: PI controller with current control loop.

$$\text{PI Controller} = K_{PC} \left[1 + \frac{1}{sT_{IC}} \right] \quad (3.14)$$

$$\text{PWM VSC} = \frac{K_C}{1 + sT_{TC}} \quad (3.15)$$

$$\text{Line Inductors} = \frac{K_{RL}}{sT_{RL} + 1} \quad (3.16)$$

$$\begin{aligned} \text{Total time delay,} \\ T_{TC} \end{aligned} = T_S + T_{PWM} + T_d \quad (3.17)$$

$$K_{RL} = \frac{1}{R} \quad (3.18)$$

$$T_{RL} = \frac{L}{R} \quad (3.19)$$

$$K_{PC} = \frac{T_{RL}}{2(T_S + T_{PWM} + T_d)K_{RL}} \quad (3.20)$$

$$T_{IC} = 4(T_S + T_{PWM} + T_d) \quad (3.21)$$

Where,

- K_{PC} - Proportional gain of the PI regulator
- T_{IC} - Integrating Time of the PI regulator
- K_C - Converter Gain
- T_{TC} - Total time delay in current controller
- V_{VSC} - Voltage of the PWM voltage source converter
- V_{dist} - Voltage disturbance
- L - Line Inductance
- R - Inductor's internal resistance
- I_{dq} - Measured line current for rotating reference frame
- $I_{dq,ref}$ - Reference current for rotating reference frame
- T_s - Sampling time
- T_{PWM} - Statistical time delay of PWM signals
- T_d - Dead time of converter

In this project, the dead time, T_d is negligible as for ideal converter, while the converter gain, K_C is assumed as 1. Besides, T_{PWM} is set equal to 0 to $2T_s$. Thus, all the equations can be validated through simulation and the result are shown in Figure 3.10.

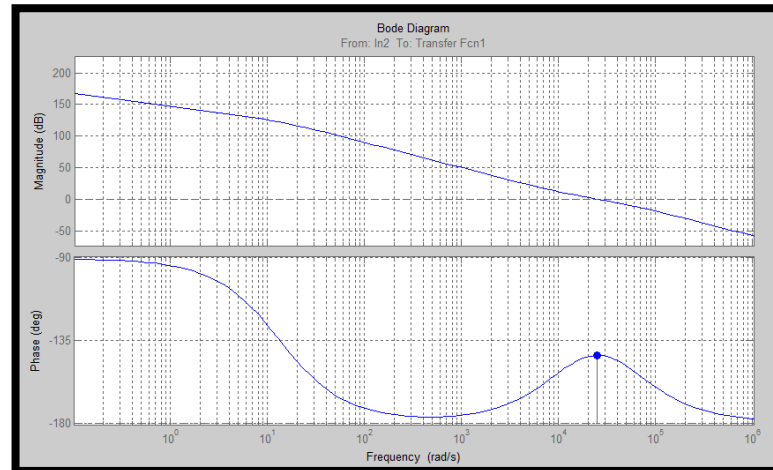


Figure 3.10: Open loop current controller bode diagram.

From the bode diagram, the phase margin is 36.9° with 25000 rad per second (rad/s) or 157.08kHz. The phase margin shown was in negative and this shows that the system is stable.

3.3.7 Inverse Park Transformation

By using the inverse park transformation, the rotating reference frame are transformed to stationary reference frame. This means that the transformation involves from dq-frames back to $\alpha\beta$ -frames as shown in Figure 3.11. $V_{conv,d}$, $V_{conv,q}$ and θ as the inputs of the transformation, while $V_{conv,\alpha}$ and $V_{conv,\beta}$ as the outputs of the transformation. The subsystem is build based on the Equations (3.8) and (3.9).

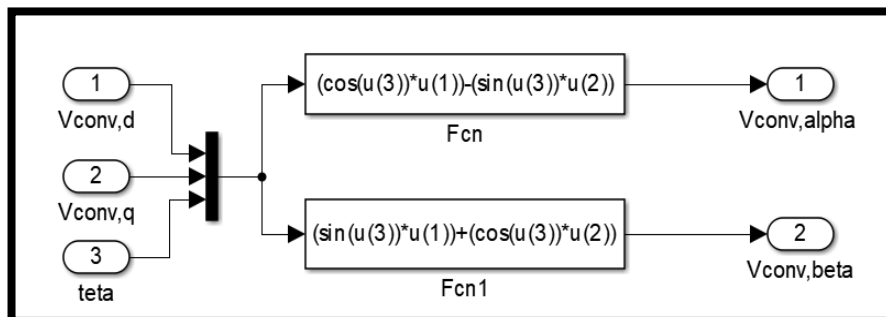


Figure 3.11: The block diagram of Inverse Park Transformation.

$$[X_\alpha] = [\cos\theta \quad -\sin\theta] [X_d] \quad (3.22)$$

$$[X_\beta] = [\sin\theta \quad \cos\theta] [X_d] \quad (3.23)$$

3.3.8 Inverse Clarke Transformation

Furthermore, there goes another transformation, known as the Inverse Clarke transformation. The transformation is from $V_{conv, d}$ and $V_{conv, q}$ as the input to $V_{conv, a}$, $V_{conv, b}$ and $V_{conv, c}$ as the output as shown in Figure 3.12. Equations (3.24), (3.25) and (3.26) are the equation being used for the transformation.

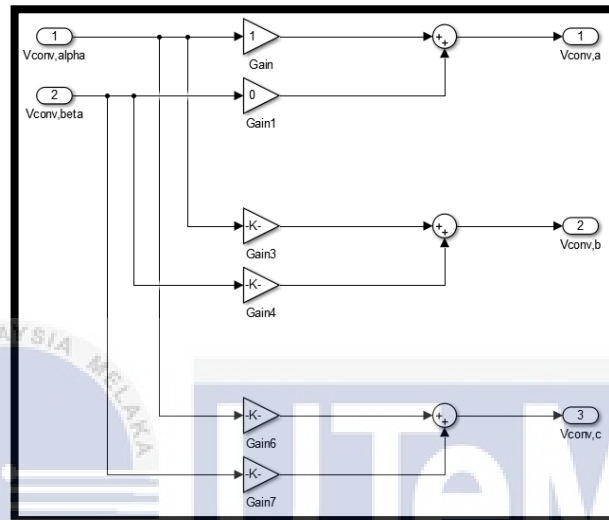


Figure 3.12: Block diagram of Inverse Clarke Transformation.

$$[V_{conv,a}] = [V_{conv,\alpha} + 0V_{conv,\beta}] \quad (3.24)$$

$$[V_{conv,b}] = \left[-\frac{1}{2}V_{conv,\alpha} + \frac{\sqrt{3}}{2}V_{conv,\beta}\right] \quad (3.25)$$

$$[V_{conv,c}] = \left[-\frac{1}{2}V_{conv,\alpha} - \frac{\sqrt{3}}{2}V_{conv,\beta}\right] \quad (3.26)$$

3.3.9 Sinusoidal Pulse Width Modulation (SPWM)

SPWM as shown in Figure 3.13 is the design that can directly control the DC output voltage and the three-phase input. After the Inverse Clarke Transformation, the output of it which is the V_{conv} , $a\ b\ c$ will act as the input of the SPWM block system. The three signals, $V_{conv,a}$, $V_{conv,b}$ and $V_{conv,c}$ will be compared with the triangular carrier wave. The carrier signal frequency in this project is set to 2050Hz. Hence, the output of the block system will be in switching pattern, which are S_a , S_b and S_c that will have fed onto the Insulated Gate Bipolar Transistor (IGBT).

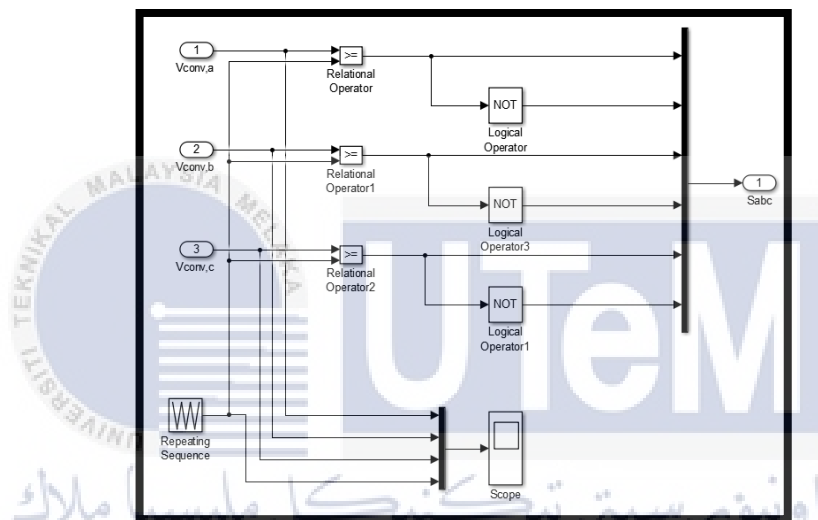


Figure 3.13: Simulink block of Sinusoidal Pulse Width Modulation.

CHAPTER 4

SIMULATION AND DISCUSSION OF RESULTS

In this chapter, the simulation results will be display which gathered from the simulation of each subsystem of block diagram in Chapter 3. In addition, the results are represented in graph through the scope in Simulink. There is discussion on the results that represented. The discussion is based on the analysis been made to compare it with the current results.

4.1 Simulation of open loop rectifier

In the beginning, before doing the complete simulation of VOC, the simulation of an open loop rectifier need to be done. Figure 4.1 shows the open loop rectifier that is run in the MATLAB.

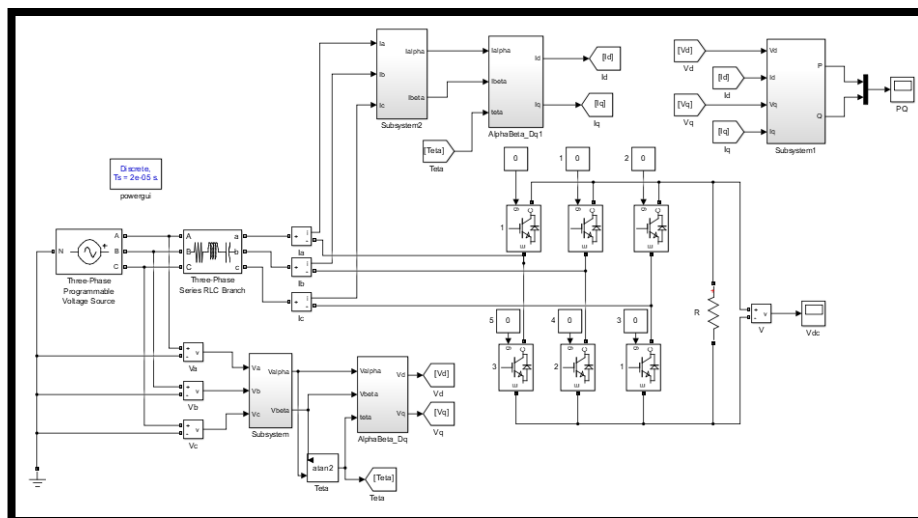


Figure 4.1: Circuit of open loop rectifier.

During the simulation of open loop rectifier, there is a transformation between stationary coordinates $\alpha\beta$ and synchronous rotating coordinates dq . This method causes the transient response to be faster with high static performance through internal current control loop. For the simulation, the $a\beta c$ -frame and $\alpha\beta$ -frame as the input voltage and current waveforms are obtained. The waveforms that display shows the relationship between them which are also known as the Clarke transformation. Figure 4.2 shows the three-phase input voltages that are transform to $\alpha\beta$ -frame that are then shown in Figure 4.3. The same pattern was used for the Clarke Transformation for currents.

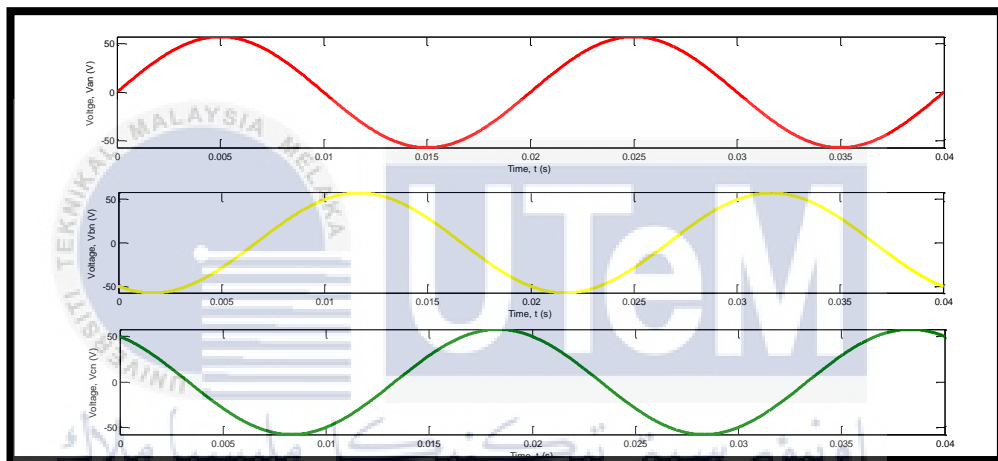


Figure 4.2: Waveform of input voltages in $a\beta c$ -frame.

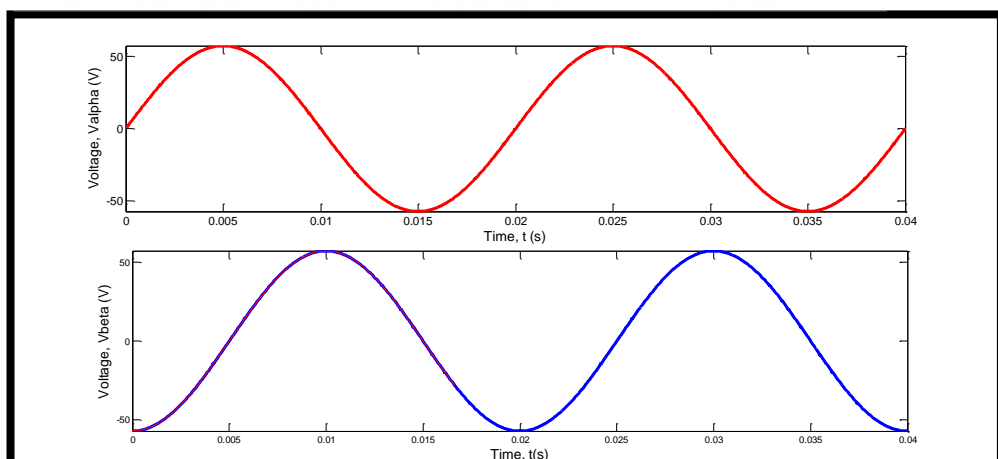


Figure 4.3: Waveform of input voltages in $\alpha\beta$ -frame.

The current waveforms shown in Figure 4.4 are non-sinusoidal as the current harmonic present in the diode rectifiers. The operation of circuit is during the open loop rectifier simulation. Hence, the current waveforms in Figure 4.5 shown after the transformation will be non-sinusoidal too.

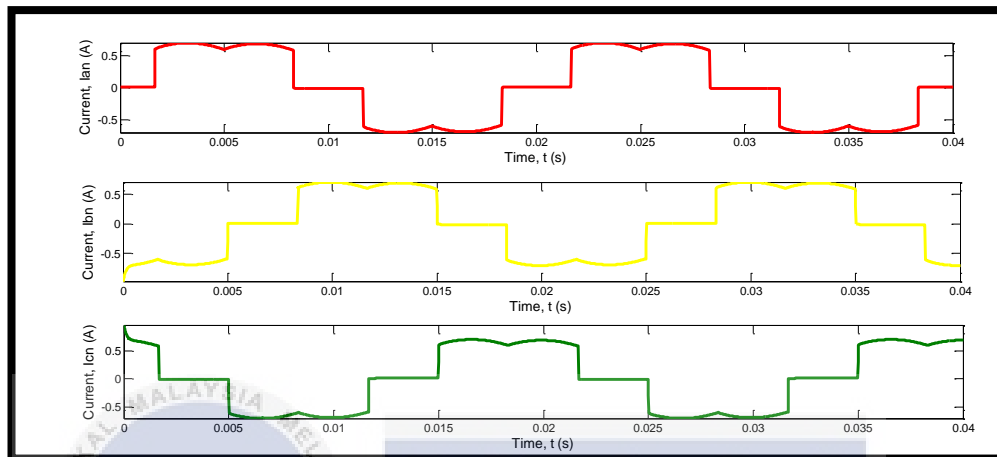


Figure 4.4 Waveform of input currents in abc-frame.

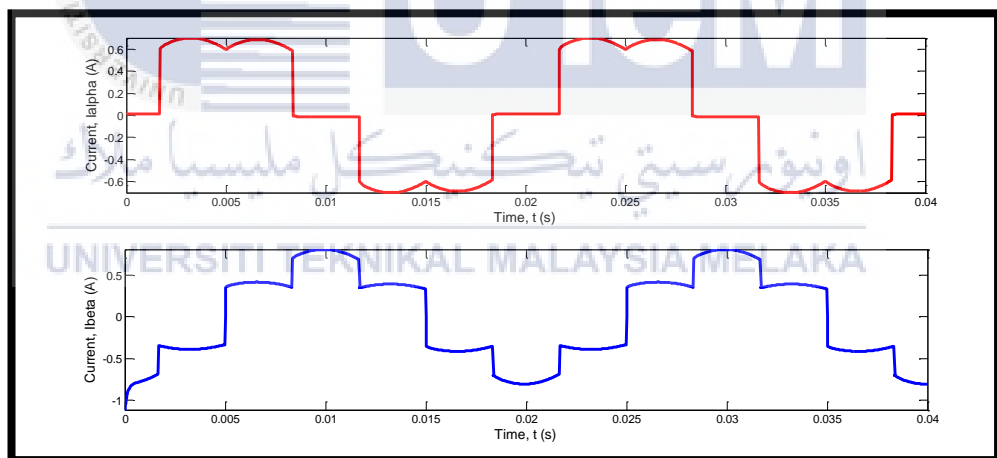


Figure 4.5 Waveform of input currents in $\alpha\beta$ -frame.

The simulation is continuing by transforming $\alpha\beta$ -frame into dq-frame by Park Transformation. This transformation also known as dq-transformation where the angle reference, θ is fed from atan2 . Other than that, Figure 4.6 shows the voltage angle of atan2 that is implemented in synchronous dq reference frame.

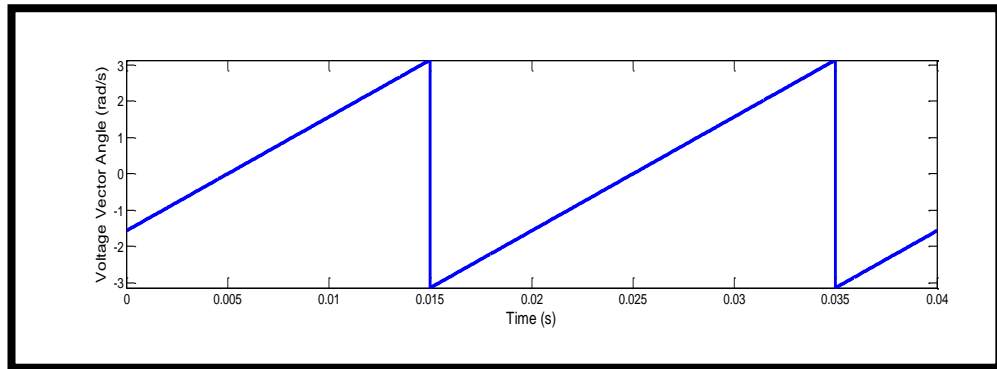


Figure 4.6: Voltage angle produced by atan2

Other than that, the simulation was tested when replace the atan2 with PLL block system in Figure 4.7. The result was compared with when using atan2 as in Figure 4.8. Hence, it shows the same waveform for either using the atan2 nor PLL.

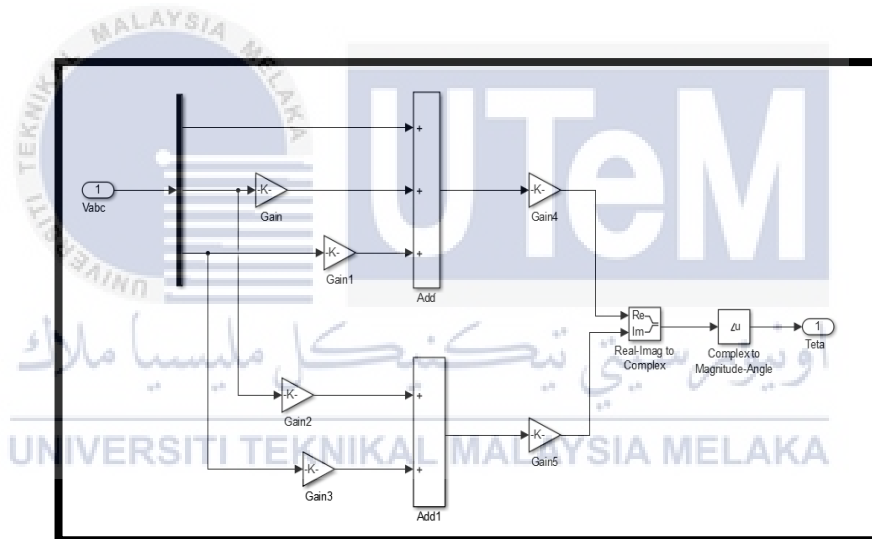


Figure 4.7: Block diagram of PLL.

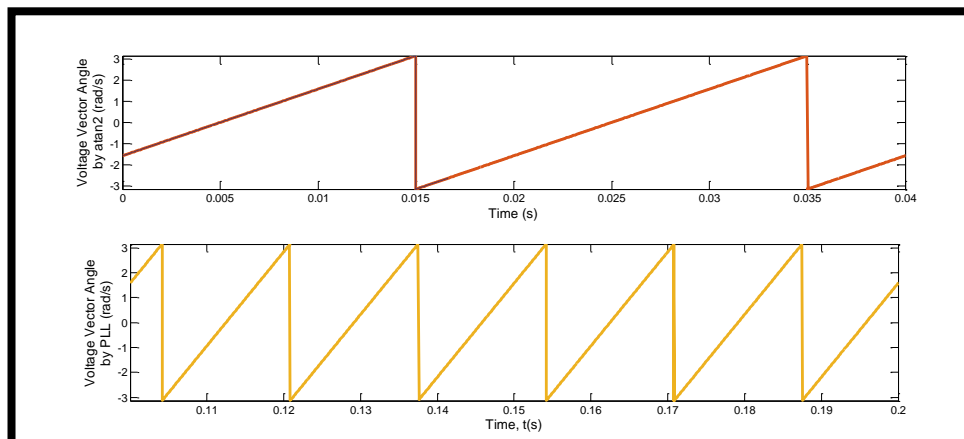


Figure 4.8: Voltage angle produced by atan2 and PLL.

A correct Park Transformation need the exact value of the angle $\theta(t)$ to be decouple the components for independent power control. In this project, atan2 was used in order synchronizing the turning on and off the power devices, calculating and controlling flow of active and reactive power by transforming the feedback variables to a reference frame suitable for control purposes.

Furthermore, atan2 is then implement in synchronous dq reference frame. Where, the Park Transformation are formed. Figure 4.9 shows the transformation of $\alpha\beta$ -frame into dq-frame for the voltages.

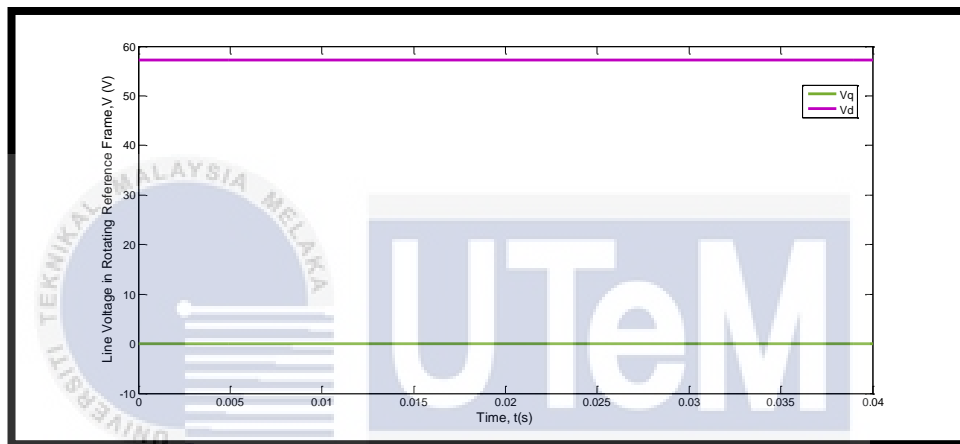


Figure 4.9: Supply voltage in synchronously rotating dq reference frame.

The voltage transformation for V_q equal to 0V and is maintain as the controller produces unity power factor operation. Next, the Park Transformation for currents was as in Figure 4.10.

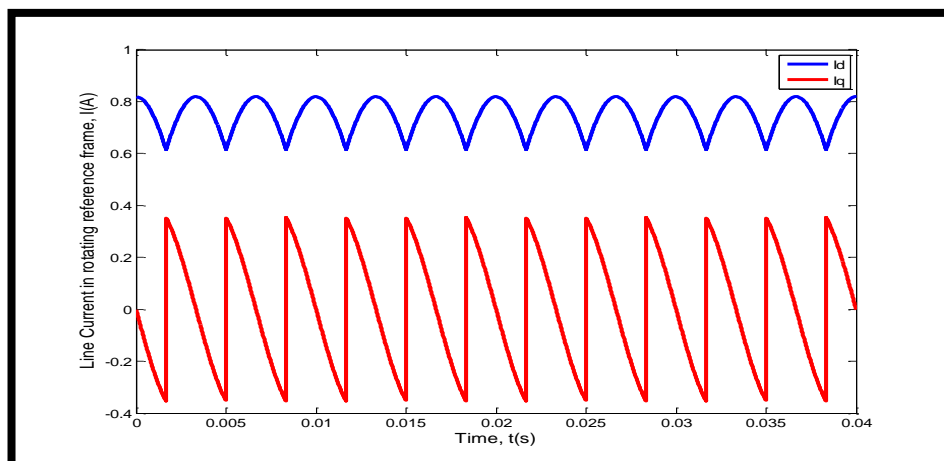


Figure 4.10: Supply current in synchronously rotating dq reference frame.

The result shows that the value of I_q are equal to 0A, but not constant along the simulation as the transformation of currents are not sinusoidal since beginning. Moreover, Figure 4.11 shows the frequency spectrum of the grid current.

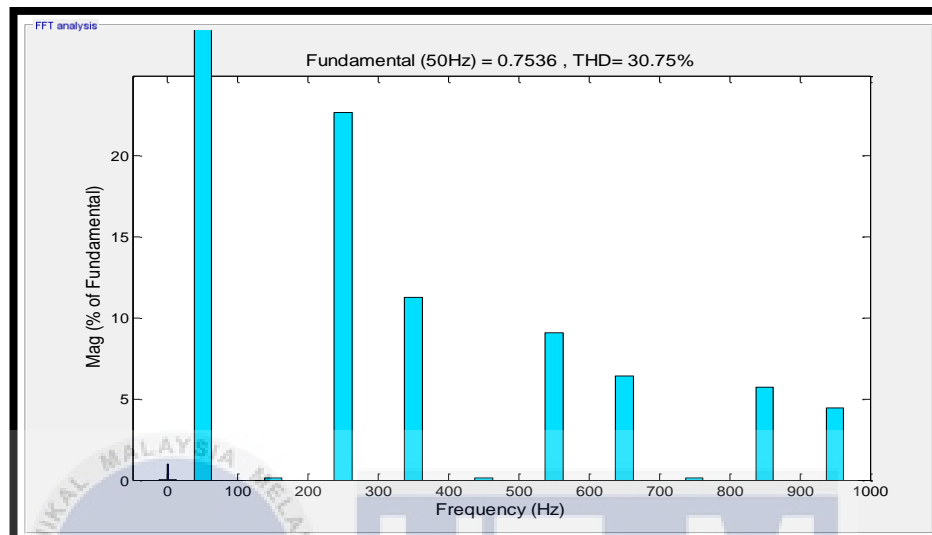


Figure 4.11: frequency spectrum of grid current.

As shown in the Figure 4.11, the Total Harmonic Distortion, THD of the grid current is 30.75% which are too high and need to be improve. While, the power flow of voltages and currents are then obtain. The value of active power, P and Reactive power, Q can be obtain through the equation as shown in Figure 4.11. The result was shown in Figure 4.12, which shows that the power flow obtained was 70.71W of active power and 70.71Var for reactive power.

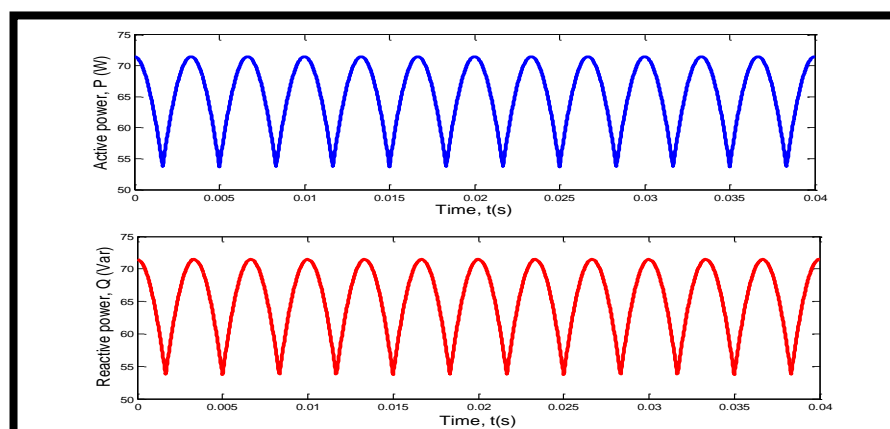


Figure 4.12: Waveform of Active power and Reactive power.

As we can see that the Active and reactive power for this system is the same as the input voltage, which are 70.71W of active power and 70.71Var of reactive power. As a result, we can see that the generated DC output voltage waveform in Figure 4.13 was sinusoidal with peak value of 99V.

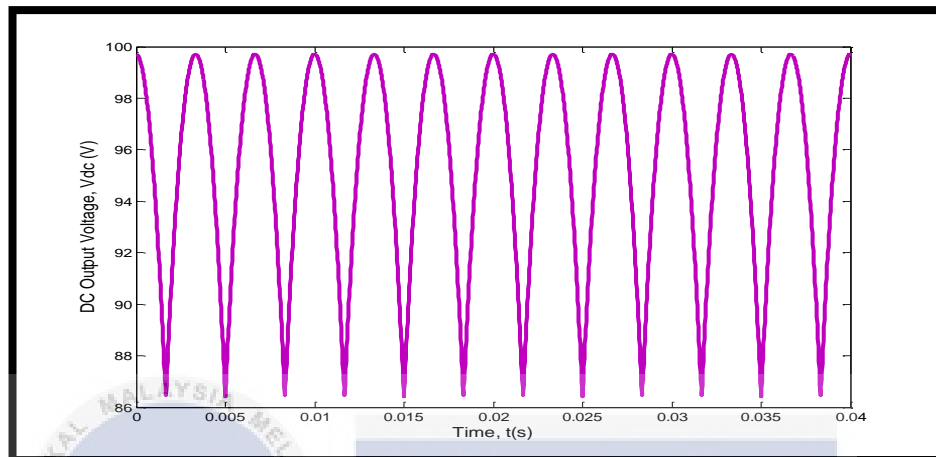


Figure 4.13: Generated dc-link output voltage.

Figure 4.14 shows the combination of input voltages and generated dc-link output voltage. The combination proves that the waveforms of input voltages together with the subsystem block of Clarke Transformation are correct. We can also see that the waveform of DC output voltage follows the three-phase input voltages.

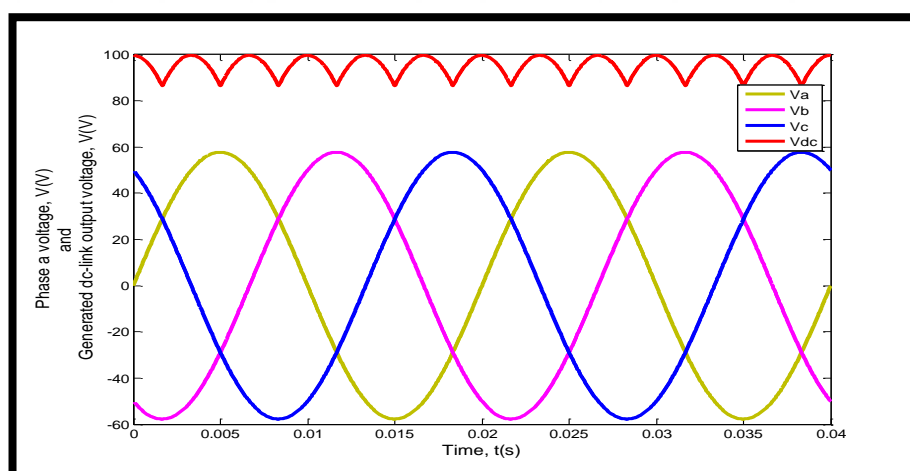


Figure 4.14: Waveform of input voltages and generated dc-link output voltage.

4.2 Simulation of three-phase AC to DC converter using VOC

In this project, a complete VOC does need decoupled controller, where a voltage controller and two current controllers was used. This is important in order having a sinusoidal waveform of line current. Figure 4.15 shows the complete structure of VOC in MATLAB. In the study, there are two types of converters, known as Voltage Source Converters (VSC) and Current Source Converters (CSC). Voltage fed converter is the VSC, while current fed converter is the CSC. VSC consists of Insulated Gate Bipolar Transistor (IGBT) that can be either turning on nor off in a controller manner.

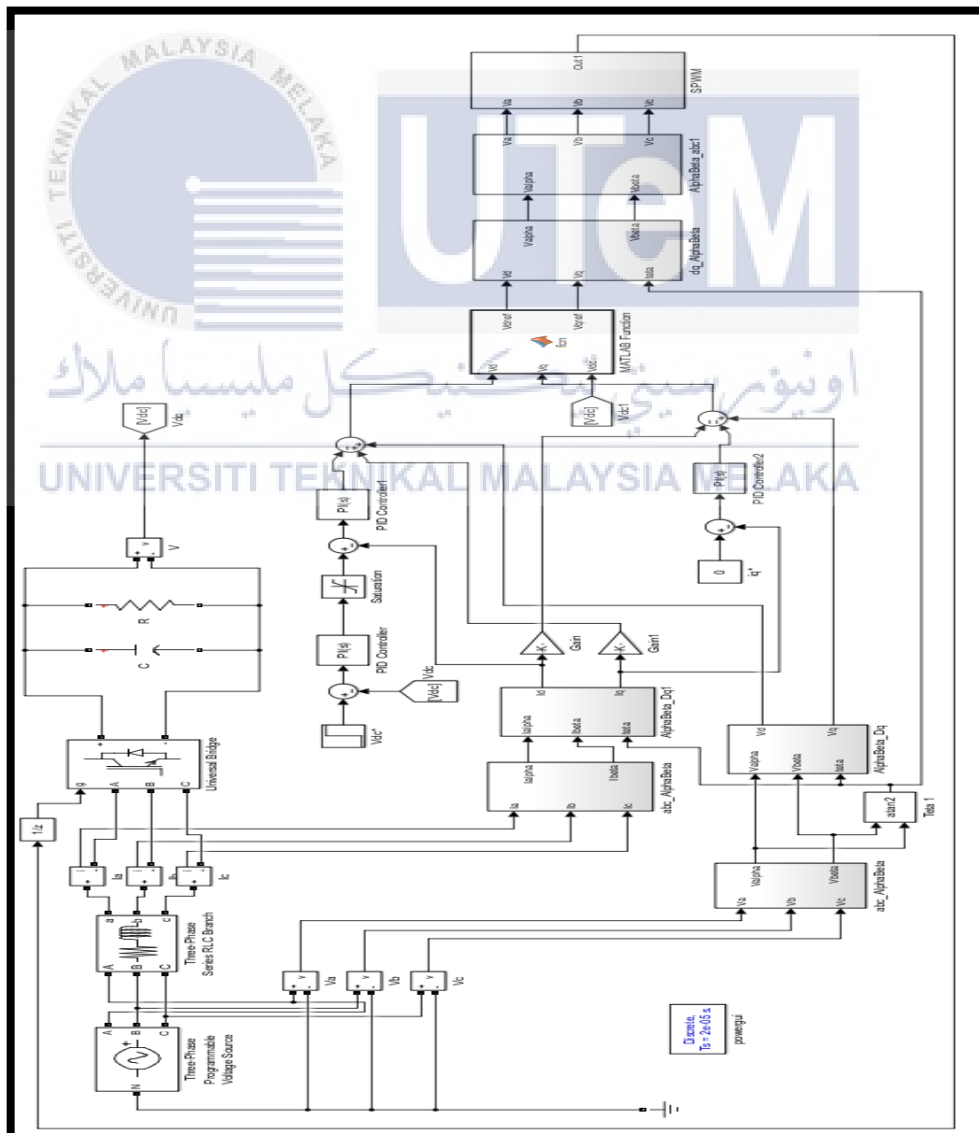


Figure 4.15: Complete structure of VOC in MATLAB.

In order determining the suitable value for both the voltage and current controller, the equations of (2.25) to (2.30) are applied. Thus, in this project, the K_{pv} is set to be equal to 67.5, while K_{iv} was set to be equal to 843750 for the voltage controller. For the current controller, the value of $K_{pi} = 375$ with $K_{ii} = 4687500$.

After implementing the decoupled controller, there are changes in the waveform of three-phase input voltages. Figure 4.16 shows that the three-phase input currents become sinusoidal form.

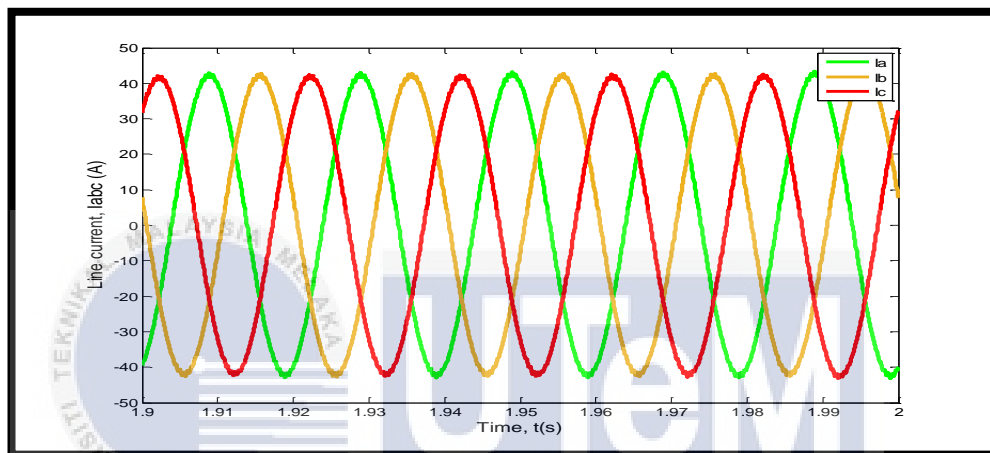


Figure 4.16: Three phase input current.

Better view on achieving the unity power factor mode, we can see through the waveform that shown in Figure 4.17.

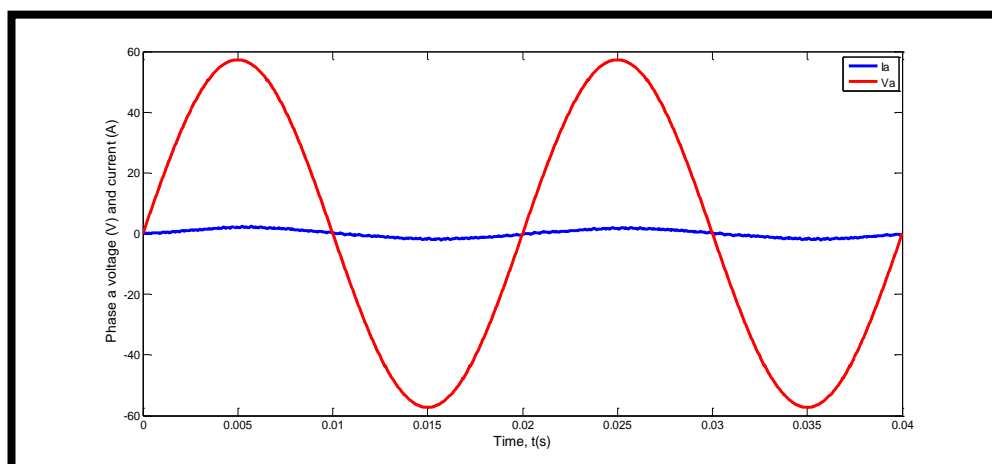


Figure 4.17: Phase a voltage and current at unity power factor.

As shown in Figure 4.17, the phase a voltage is in phase with phase a current. This shows during the unity power factor mode. In addition, Figure 4.18 shows the line current harmonics spectrum analysis produced 0.90% of Total Harmonic Distortion (THD) with fundamental frequency of 42.03Hz. Hence, we can see that by implementing the decoupled controller, we can obtain a low THD current value.

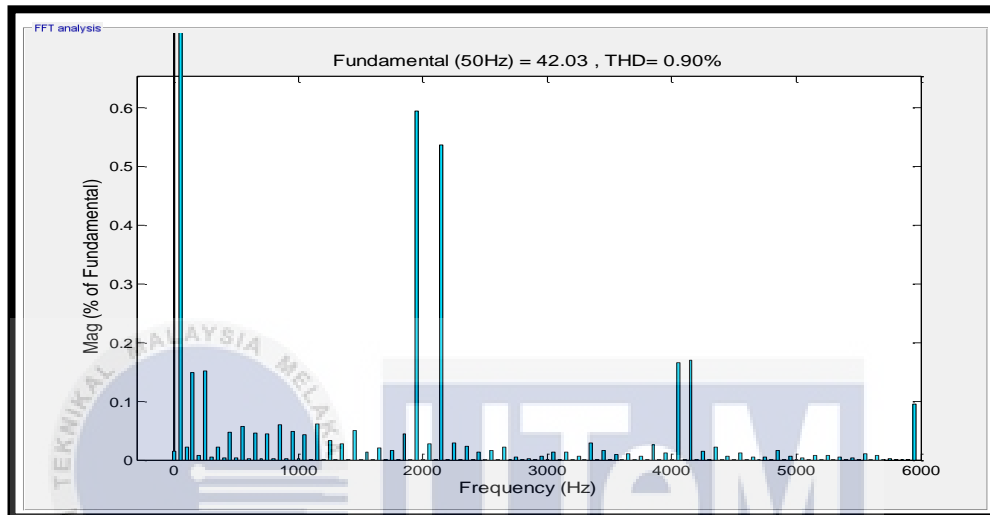


Figure 4.18: Frequency spectrum of line current.

In addition, the line current in rotating dq-reference frame was shown in Figure 4.19. As we can see from the figure, the value of I_q was maintained at -40A, while the value of I_d was maintained at 17A.

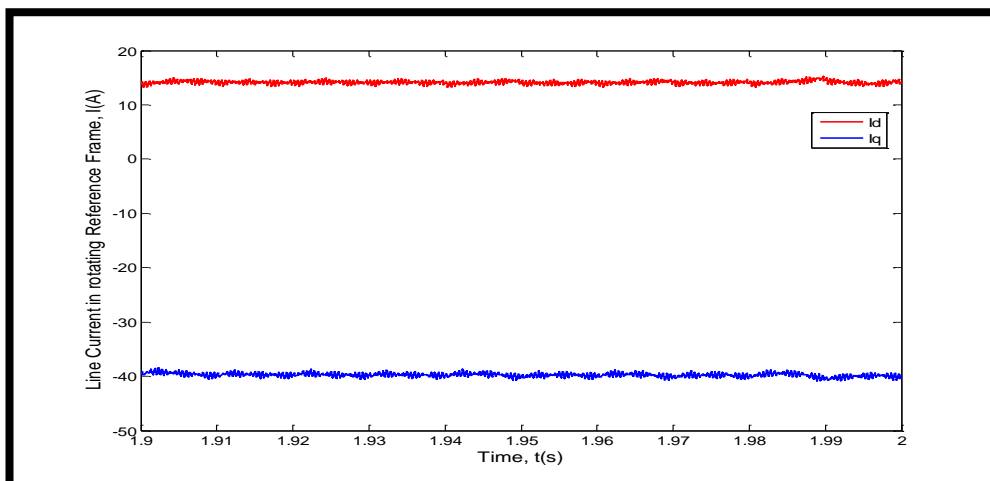


Figure 4.19: Supply current in synchronously rotating dq-reference frame.

The output of the controllers is voltage converter d, $V_{\text{conv}, d}$ and voltage converter q, $V_{\text{conv}, q}$. The output voltages are normalised between 1V and -1V using the MATLAB function. The simulation was continued with the inverse Park transformation and inverse Clarke transformation to have an output of three-phase voltage converter, $V_{\text{conv}, abc}$.

After implementation of decoupled controller, we can see that there are changes in the active and reactive power as shown in Figure 4.20.

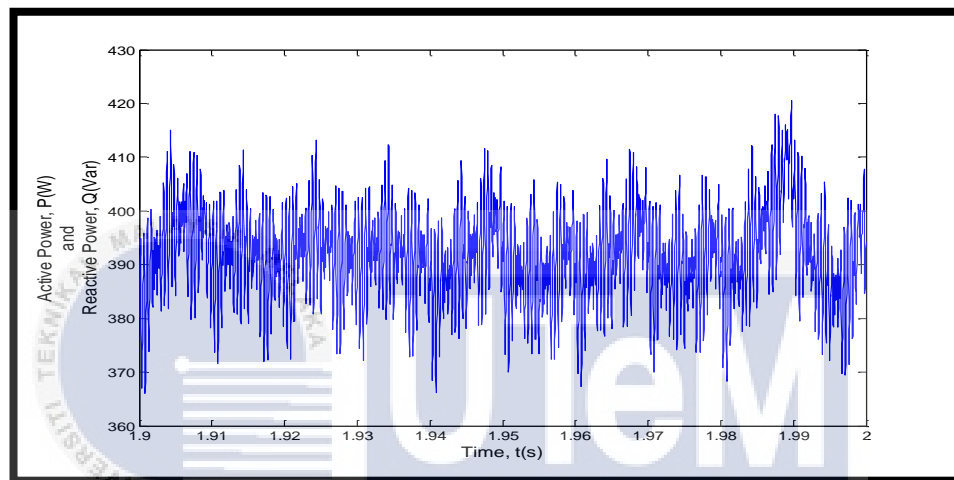


Figure 4.20: Active and reactive powers of system.

The value of active and reactive powers become $400W+j400Var$. Lastly, Figure 4.21 show the dc-link output voltage of the system.

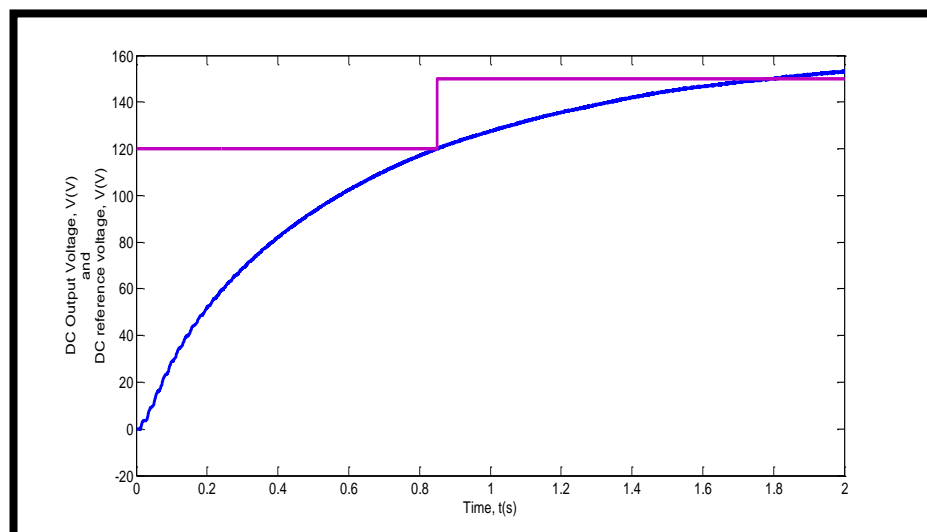


Figure 4.21: DC-link output voltage with reference voltage.

As we can see from the Figure 4.21, the dc output voltage has almost same shape as the reference voltage.

4.3 Power Factor Operation Modes

In this project, the system is test with difference value of reactive power. In this work, the Q_{ref} is set to be equal to 100Var. Figure 4.22 shows the changes that occur on the line current in dq frames.

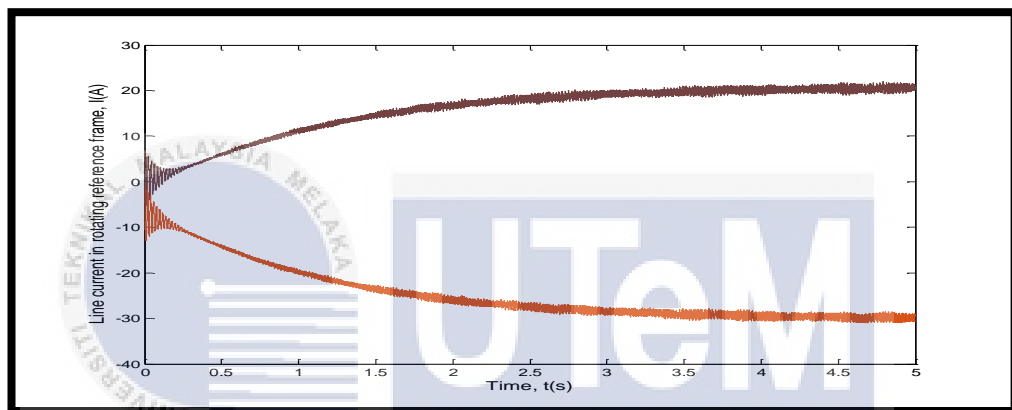


Figure 4.22: Line current in dq-frame with $Q_{ref} = 100\text{Var}$

The line current rotating frame was affected by the changes value of reference reactive power. Figure 4.22 shows that the I_q is shifting down towards greater negative value. Hence, this will cause the lagging power factor as the phase a current, I_a lag the phase a voltage, V_a as shown in Figure 4.23 below.

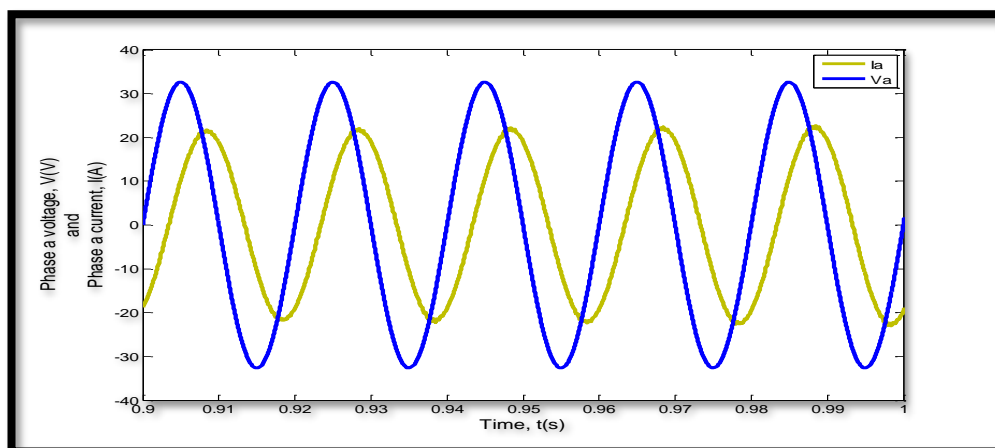


Figure 4.23: Phase a voltage and phase a current.

Other than that, the value of Q_{ref} is set to -100Var . Figure 4.24 shows the changes occur.

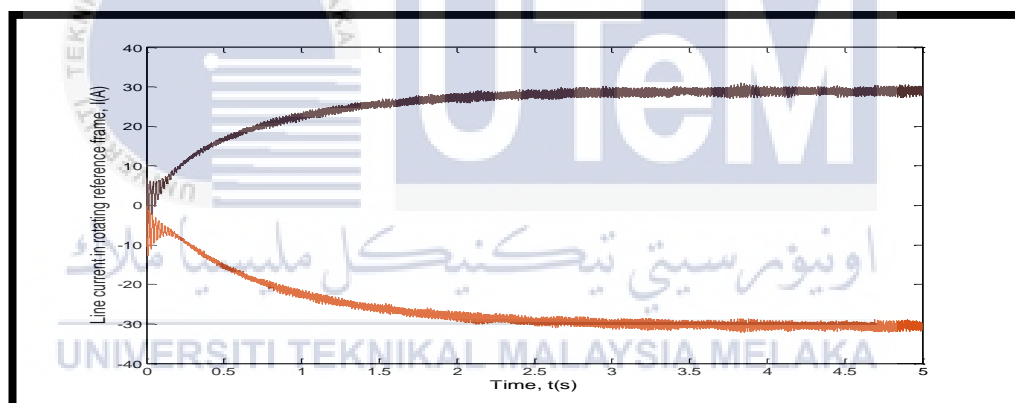


Figure 4.24: Line current in dq-frame with $Q_{ref} = -100\text{Var}$.

As shown in Figure 4.24, the value of I_d is move towards positive value. This causes the leading of power factor as the phase a current, I_a leads the phase a voltage, V_a as shown in Figure 4.25 below.

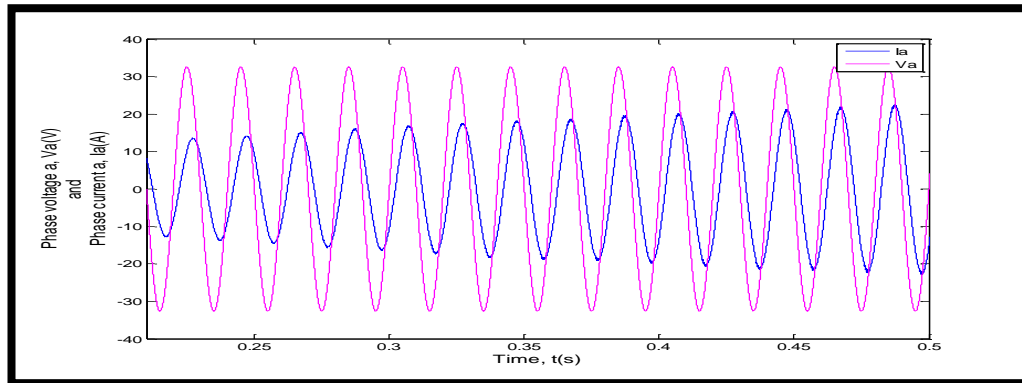


Figure 4.25: Phase a voltage with phase a current.

4.4 Dynamic Performance

4.4.1 Load Variation

The performance of VOC was tested by testing the dynamic performance during variation of load and changes in DC voltage output reference. Figure 4.26 shows the simulation diagram of VOC with a load variation. At first, the resistor with 100Ω was connected in parallel with the existing resistor. The setting time in the breaker is set to 1s.

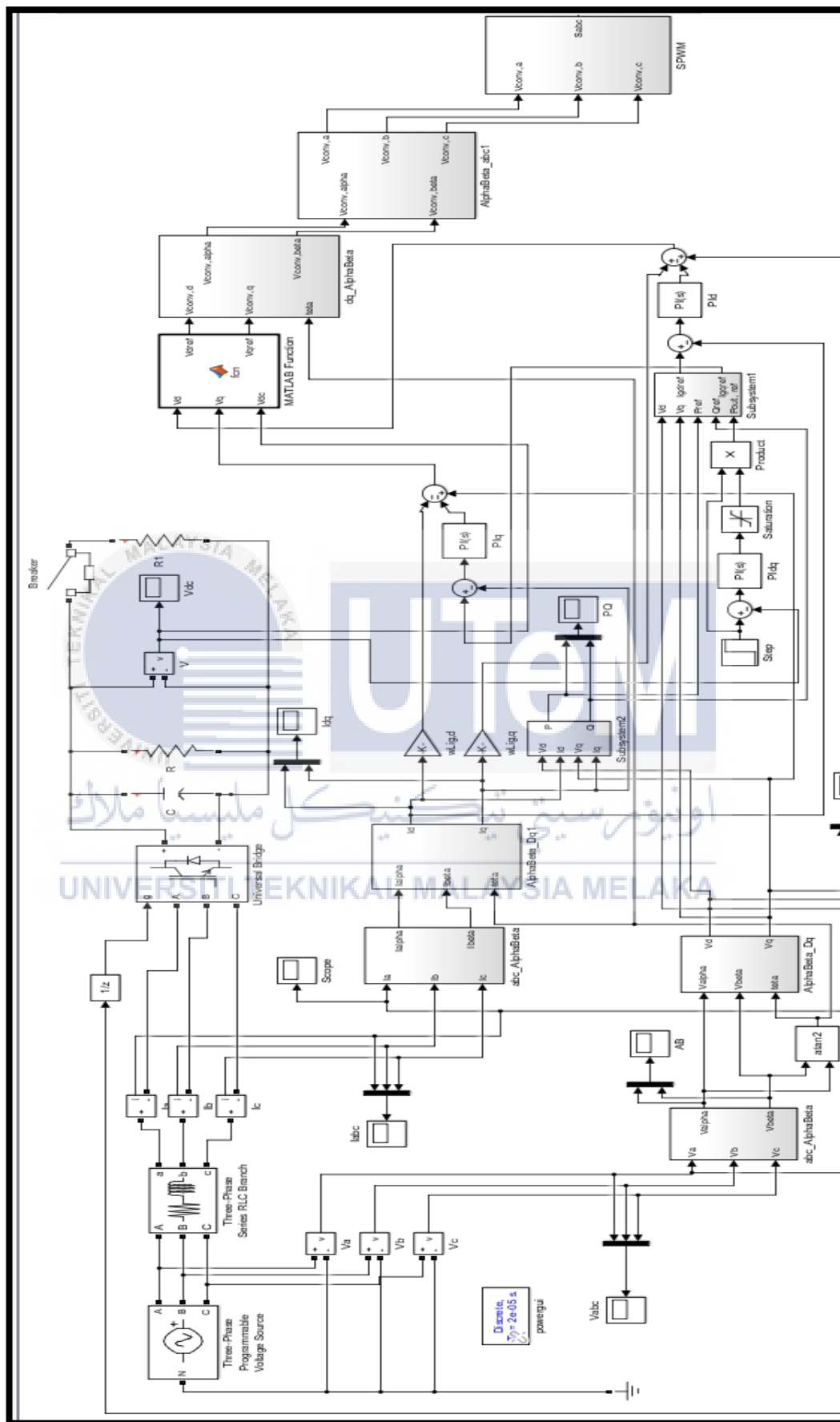


Figure 4.26: VOC with load variation

Figure 4.27 shows that there are changes as the load is connected in parallel to the existing resistance. As we can see that during the time at 1s, the output voltage was increased to 140V and then back to 100V after 1s.

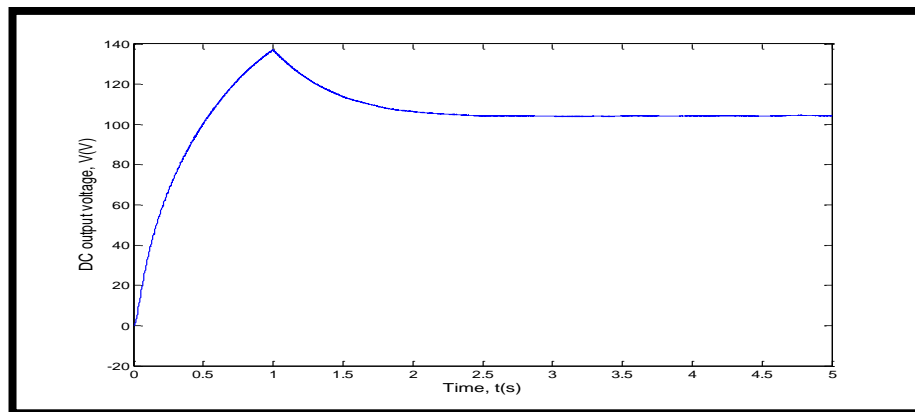


Figure 4.27: DC-link output voltage with 100 Ω of resistor in parallel.

The rotating frame of I_{dq} also been disturbed during the time at 1s and then back to normal value of current after the 1s as shown in Figure 4.28.

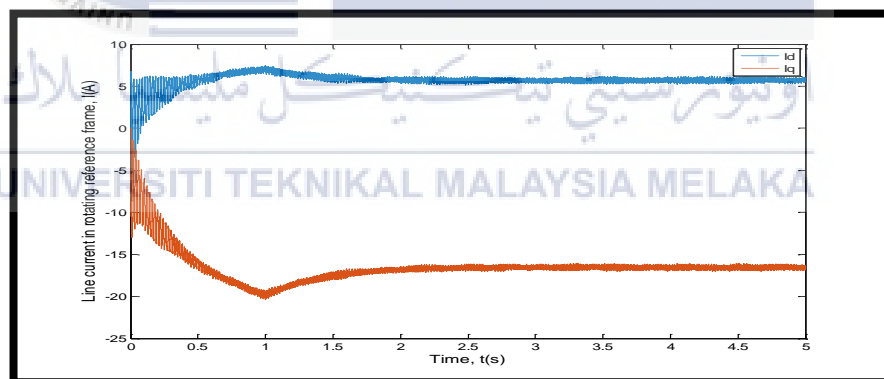


Figure 4.28: Line current in rotating frame with 100 Ω in parallel.

Figure 4.29 shows the performance of phase current a, I_a along the setting time. The value of I_a is less in the beginning, but it started increase after 1s. This is due to the load variation and resistor that connected with each other. Therefore, the output voltage was disturbed during the time at 1s.

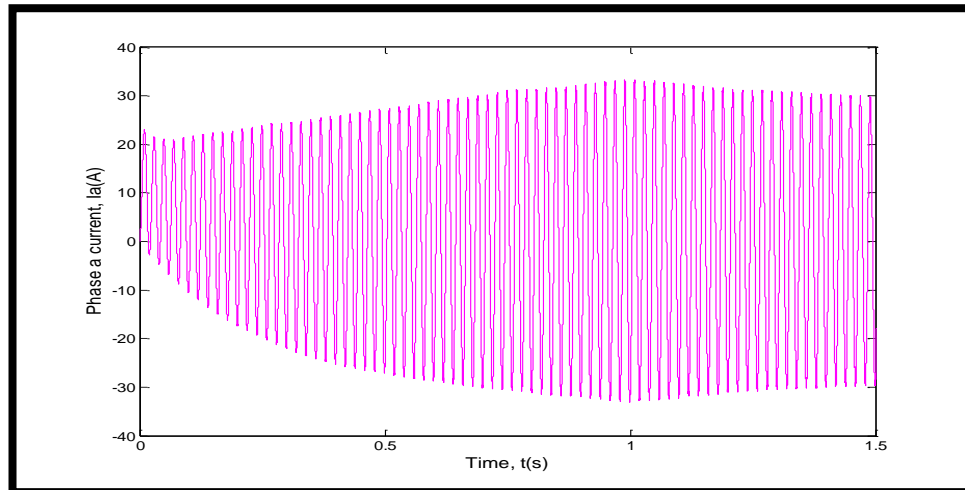


Figure 4.29: Phase a current with 100Ω in parallel.

Finally, we can see in Figure 4.30, where the active power is also increase to around 250W at 1s. The active power was affected due to the presence of 100Ω of resistor that was connected in parallel with existing resistor.

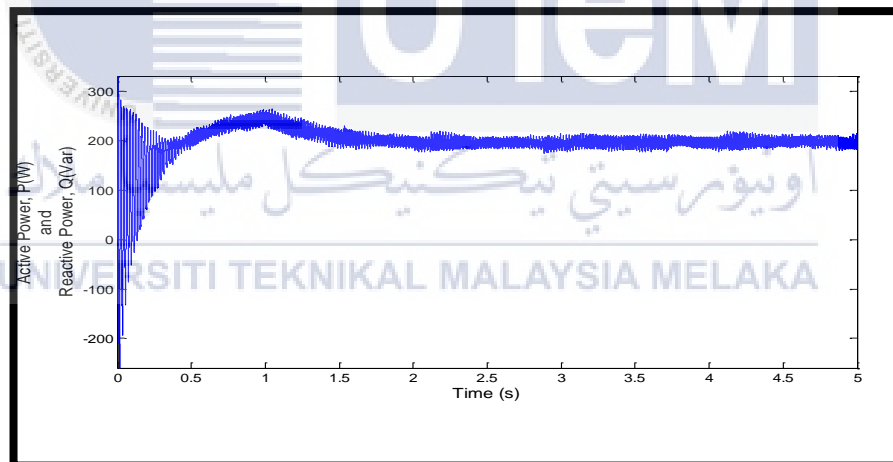


Figure 4.30: Power flow of system with 100Ω in parallel.

In addition, the project is continuing by changing the load variation from 100Ω to 200Ω . During the experiment, the output voltage of the system overshoot at 1s as shown in Figure 4.31. The overshoot was lower than during the load variation at 100Ω .

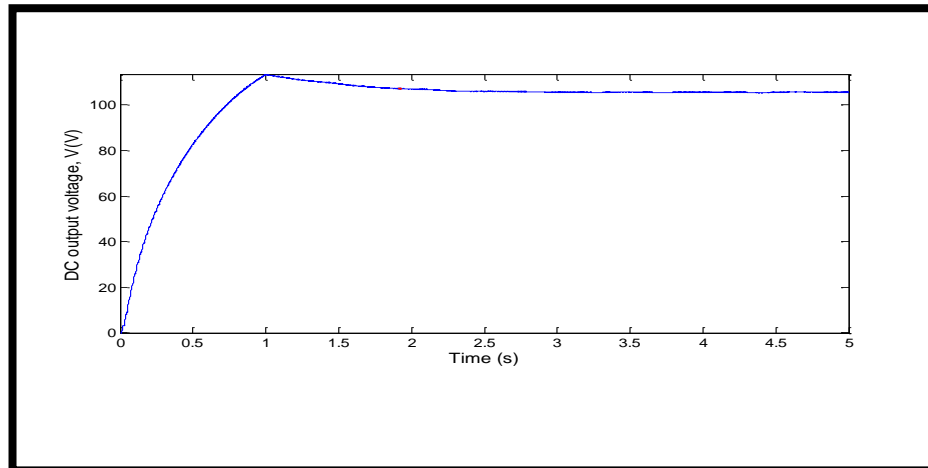


Figure 4.31: DC-link output voltage with 200 Ω of resistor in parallel.

From the Figures of 4.32, 4.33 and 4.34, we can see that at 1s, there are changes that occur after a 200 Ω of resistor that was connected in parallel with the existing resistor. As in Figure 4.32, we can see that the value of I_q move downward toward negative value at 1s.

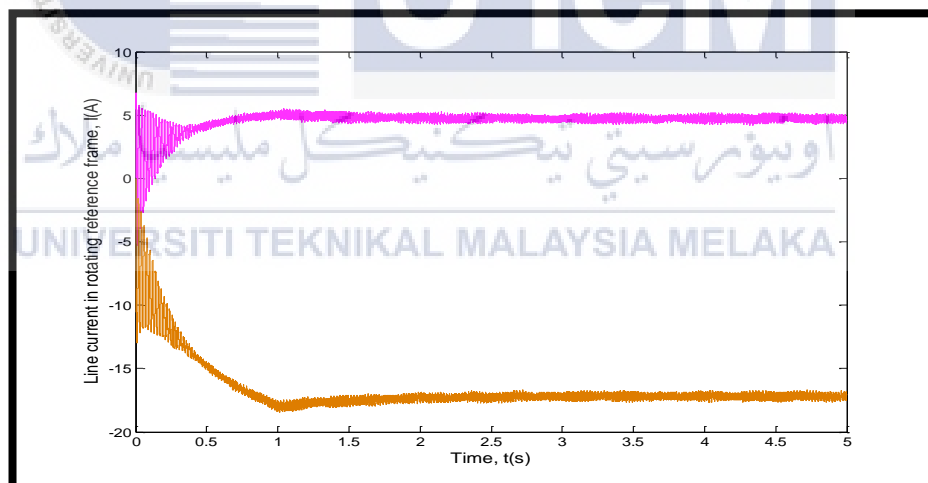


Figure 4.32: Line current in rotating frame with 200 Ω in parallel.

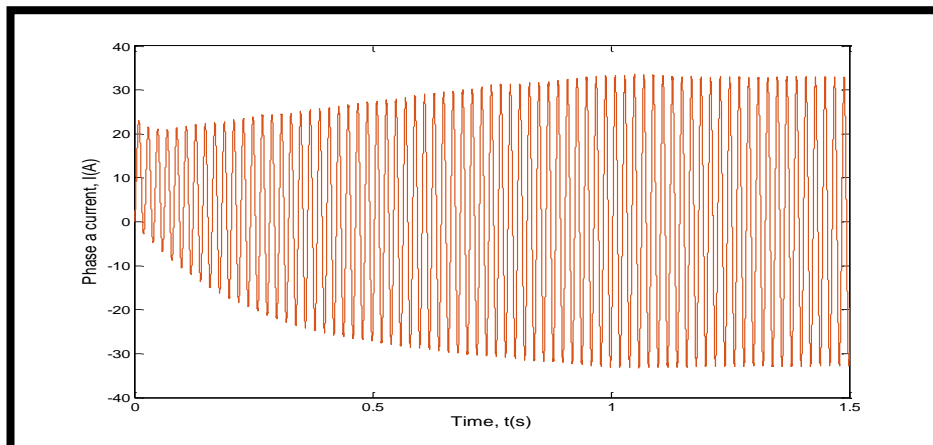


Figure 4.33: Phase a current with 200 Ω in parallel.

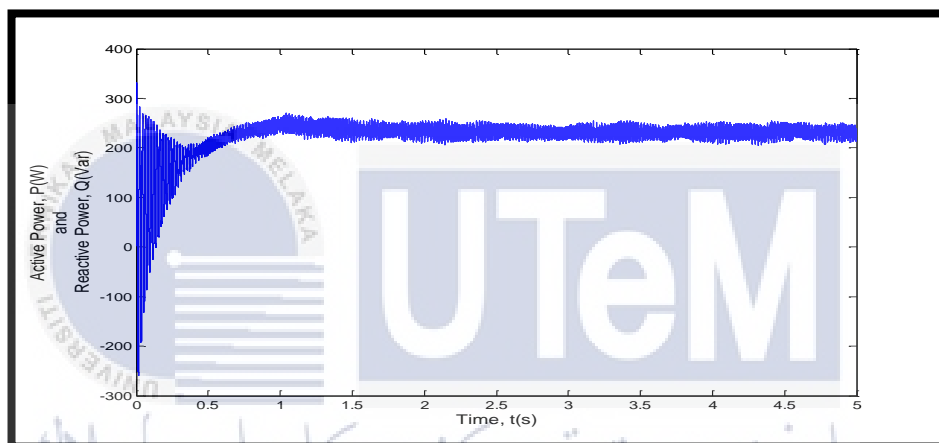


Figure 4.34: Power flow of system with 200 Ω in parallel.

CHAPTER 5

CONCLUSION AND RECOMMENDATION

In this chapter, it will summarize all the work or method being used in this project. Any recommendation that should be made for future work is stated clearly in this chapter.

5.1 Conclusion

As a conclusion, the scope of power electronic in the industry are large and keep expands as people keep explore it more and more. In this project, it shows one of the method that been use in order making the work in industry to be smooth.

During the study on the performance of AC to DC converter, there is a few techniques that can be using to control the signal produce. Each of the technique have its' own strengthens and weaknesses in their certain part. This project is focus more on VOC method in order controlling the signal produce.

VOC is one of the method that can give a better performance through the internal current control loop. Although the process is complex, but it can give a power factor nearest to unity. In addition, the switching frequency is fixed, where the rate at which the DC voltage during switch is ON and OFF is fixed. This process is done when the pulse width modulation in the switching power supply is being process too.

Throughout the study, a complete VOC can be design and simulate using MATLAB. Besides, by implementing the decoupled control, it helps to lower the THD value of the grid current. In addition, the grid current also able to have almost sinusoidal waveform with almost equal to unity power factor. In a nutshell, by using VOC method, the DC output voltage is close to the reference voltage.

5.2 Recommendation on Future Work

In this project, it is about the analysis on grid connected front end AC to DC converter by using Voltage Oriented Control method. The steady-state response of the three-phase diode rectifier and after the implementation of VOC. Hence, it is recommended to compare the simulation results with the hardware results. It is required in order proving all the waveforms either before nor after implementing the decoupled controller.

Other than that, it can directly help in understanding more on why and how the flow of the project should be. In addition, it is recommended to study more on the equations of the PI controller in order having the best value of K_p and K_i during tuning the controller. This is important as it effect on the dc-link output voltage. The controller will affect the THD value in the line current, so does the power factor of the system.

In addition, in order improving the system of VOC, it is recommended to use PWM converter with dSPACE 1103 based control platform. This will help to obtain a low THD of grid current with the current sequences remains unchanged. This is because the system does not affect on the grid voltage distortions as voltage dips and harmonics. Finally, the flow and conduction of this project is shown in Appendix A.

REFERENCES

- [1] K. M. P., B. F. and K. R., "Control in Power Electronics," Elsevier Science, USA, 2002.
- [2] L. J. Yan, "Analysis and Development of A Regulated DC Power Supply Utilizing three phase AC to DC Converter," Faculty of Electrical Engineering, UTeM, Melaka, 2017.
- [3] Microsemi, "Park, Inverse Park and Clarke, Inverse Clarke Transformation," Inverse Clarke Transformation MSS Software Implementations User Guide, 2013. [Online]. Available: https://www.microsemi.com/document-portal/doc_view/132799-park-inverse-park-and-clarke-inverse-clarke-transformations-mss-software-implementation-user-guide. [Accessed 16 December 2017].
- [4] M. Malinowski, "A Comparative Study of Control Techniques for PWM Rectifiers in AC Adjustable Speed Drives," *IEEE Transactions on Power Electronics*, vol. 18, p. 1390, 2003.
- [5] J. Holz, "Pulsewidth Modulation," *IEEE Transactions on Power Electronics*, vol. 39, pp. 410-420, 1992.
- [6] B. -H. Kwon, "A Line-Voltage-Sensorless Synchronous Rectifier," *IEEE Transactions on Power Electronics*, vol. 14, p. 966, 1999.

- [7] X. Z. Y. J. W. H. H. Zhou, *A Novel Switching Table for Direct Power Control of Three-Phase PWM Rectifier*, 2014.
- [8] I. Poole, "PLL Phase Locked Loop Tutorial," RF Technology & Design, 14 December 2017. [Online]. Available: <http://www.radio-electronics.com/info/fr-technology-design/pll-synthesizers/phase-locked-loop-tutorial.php>.. [Accessed 16 December 2017].
- [9] H. Lennart, "Control of Variable-Speed Drives," in *Applied Signal Processing and Control*, Sweden, Department of Electronics, Malardalen University, 2002, p. 194.
- [10] J.-W. Choi, "Fast Current Controller in Three-phase AC/DC Boost Converter Using d-q Axis Crosscoupling," *Introduction*, vol. 13, p. 179, 1998.
- [11] T. Kalitjuka, "Control of voltage Source Converters for Power System Applications," Norwegian University of Science and Technology, Norway, 2011.

